Journal of Medicinal Chemistry

Article

Discovery of Clinical Candidate 4-[2-(5-Amino-1H-pyrazol-4-yl)-4-chlorophenoxy]-5-chloro-2-fluoro-N-1,3-thiazol-4-ylbenzenesulfonamide (PF-05089771): Design and Optimization of Diaryl Ether Aryl Sulfonamides as Selective Inhibitors of NaV1.7

Nigel Alan Swain, Dave Batchelor, Serge Beaudoin, Bruce M. Bechle, Paul A Bradley, Alan D Brown, Bruce Brown, Ken J Butcher, Richard P Butt, Mark L Chapman, Stephen Denton, David Ellis, Sebastien Galan, Stephen M Gaulier, Ben S Greener, Marcel J. de Groot, Mel S Glossop, Ian K Gurrell, Jo Hannam, Matthew S Johnson, Zhixin Lin, Christopher J Markworth, Brian E Marron, David S Millan, Shoko Nakagawa, Andy Pike, David Printzenhoff, David J Rawson, Sarah J Ransley, Steven M Reister, Kosuke Sasaki, R Ian Storer, Paul Anthony Stupple, and Christopher W West

J. Med. Chem., **Just Accepted Manuscript** • DOI: 10.1021/acs.jmedchem.7b00598 • Publication Date (Web): 06 Jul 2017

Discovery of Clinical Candidate 4-[2-(5-Amino-1H-pyrazol-4-yl)-4-chlorophenoxy]-5-chloro-2-fluoro-N-1,3-thiazol-4-ylbenzenesulfonamide (PF-05089771): Design and Optimization of Diaryl Ether Aryl Sulfonamides as Selective Inhibitors of $Na_V1.7$

Nigel. A. Swain,[*,a,†] *Dave Batchelor,*[e] *Serge Beaudoin,*[d] *Bruce M. Bechle,*[c] *Paul A. Bradley,*[e] *Alan D. Brown,*[a] *Bruce Brown,*[e] *Ken J. Butcher,*[e] *Richard P. Butt,*[a] *Mark L Chapman,*[d] *Stephen Denton,*[e] *David Ellis,*[e] *Sebastien Galan,*[e] *Steven M. Gaulier,*[e] *Ben S. Greener,*[e] *Marcel J. de Groot,*[e] *Mel S. Glossop,*[e] *Ian K. Gurrell,*[f] *Jo Hannam,*[e] *Matthew S. Johnson,*[d] *Zhixin Lin,*[d] *Christopher J. Markworth,*[d] *Brian E. Marron,*[d] *David S. Millan,*[e] *Shoko Nakagawa,*[e] *Andy Pike,*[b,†] *David Printzenhoff,*[d] *David J. Rawson,*[e] *Sarah J. Ransley,*[e] *Steven M. Reister,*[d] *Kosuke Sasaki,*[e] *R. Ian Storer,*[a,†] *Paul A. Stupple,*[e] *Christopher W. West,*[d].

[a]Worldwide Medicinal Chemistry, [b]Pharmacokinetics, Dynamics and Metabolism, Pfizer Ltd, The Portway, Granta Park, Cambridge, CB21 6GS, UK. [c]Worldwide Medicinal Chemistry, Pfizer Inc, Eastern Point Road, Groton, Connecticut 06340, USA. [d]Icagen Inc, 4222 Emperor Blvd # 350, Durham, NC 27703, USA. [e]Worldwide Medicinal Chemistry, [f]Pharmacokinetics, Dynamics and Metabolism, Pfizer Ltd, Ramsgate Road, Sandwich, Kent, CT13 9NJ, UK.

KEYWORDS. $Na_V1.7$, pain, sodium channel, $Na_V1.5$, CYP2C9 inhibition, microdose, aryl sulfonamide

ABSTRACT

A series of acidic diaryl ether heterocyclic sulfonamides that are potent and sub-type selective $Na_V1.7$ inhibitors is described. Optimization of early lead matter focused on removal of structural alerts, improving metabolic stability and reducing cytochrome P450 inhibition driven drug-drug interaction concerns to deliver the desired balance of preclinical in vitro properties. Concerns over non-metabolic routes of clearance, variable clearance in pre-clinical species and subsequent low confidence human pharmacokinetic predictions led to the decision to conduct a human microdose study to determine clinical pharmacokinetics. The design strategies and results from pre-clinical PK and clinical human microdose PK data are described leading to the discovery of the first sub-type selective $Na_V1.7$ inhibitor clinical candidate PF-05089771 (**34**) which binds to a site in the voltage sensing domain.

INTRODUCTION

Voltage-gated sodium channels control the flow of sodium ions across cellular membranes and are critical to the initiation and propagation of electrical impulses in excitable cells. There are nine different human isoforms of sodium channels ($Na_V1.1$-$Na_V1.9$) with varying tissue expression patterns in neurons, cardiac and skeletal muscle.[1] Several neuronally expressed sodium channels have been linked to aberrant action potential firing associated with pain and sodium channel inhibition has served as a point of pharmacological intervention in pain management.[2] Indeed, non-selective Na_V inhibitors such as lidocaine (**1**), mexilitine (**2**) and

carbamazepine (**3**) demonstrate clinical efficacy for chronic pain (Figure 1). However, these agents are of limited clinical utility due to dose-limiting side effects associated with modulation of non-pain-related Na_V sub-types.[3]

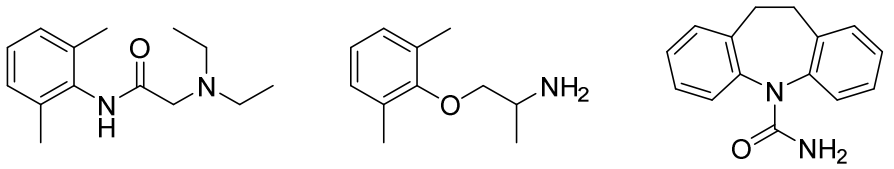

Lidocaine (**1**) Mexilitine (**2**) Carbamazepine (**3**)

Figure 1. Selected examples of sodium channel inhibitors in clinical use.

Whilst several Na_V sub-types have been implicated as potential targets in reduction of pain the most compelling human genetic evidence indicates $Na_V1.7$ as critical for pain perception.[4] Loss-of-function mutations in the SCN9a gene (which encodes $Na_V1.7$) result in the rare genetic condition, congenital insensitivity to pain (CIP).[5] Conversely, gain-of-function mutations of SCN9a can lead to extreme pain conditions such as paroxysmal extreme pain disorder (PEPD) and peripheral erythromelalgia (PE).[6]

This human genetic evidence has prompted the search for sub-type selective inhibitors of the $Na_V1.7$ channel as superior analgesics with a significantly reduced side-effect burden compared with pan-Na_V blockade.[7]

We pioneered work which identified novel lead matter containing an aryl sulfonamide acid isostere with superior sub-type selectivity particularly over the cardiac channel $Na_V1.5$ (inhibition of which may lead to arrhythmias).[8] Elegant mutagenesis studies suggested molecules such as **5** (PF-04856264) bind to a unique site in the voltage sensor domain IV which is distinct from the local anesthetic and tetrodotoxin (**4**) pore binding sites (Figure 2).[9] The

existence of this novel binding site has recently been confirmed by a X-ray crystal structure of a chimeric human $Na_V1.7$ voltage sensor domain IV in complex with an aryl sulfonamide.[10]

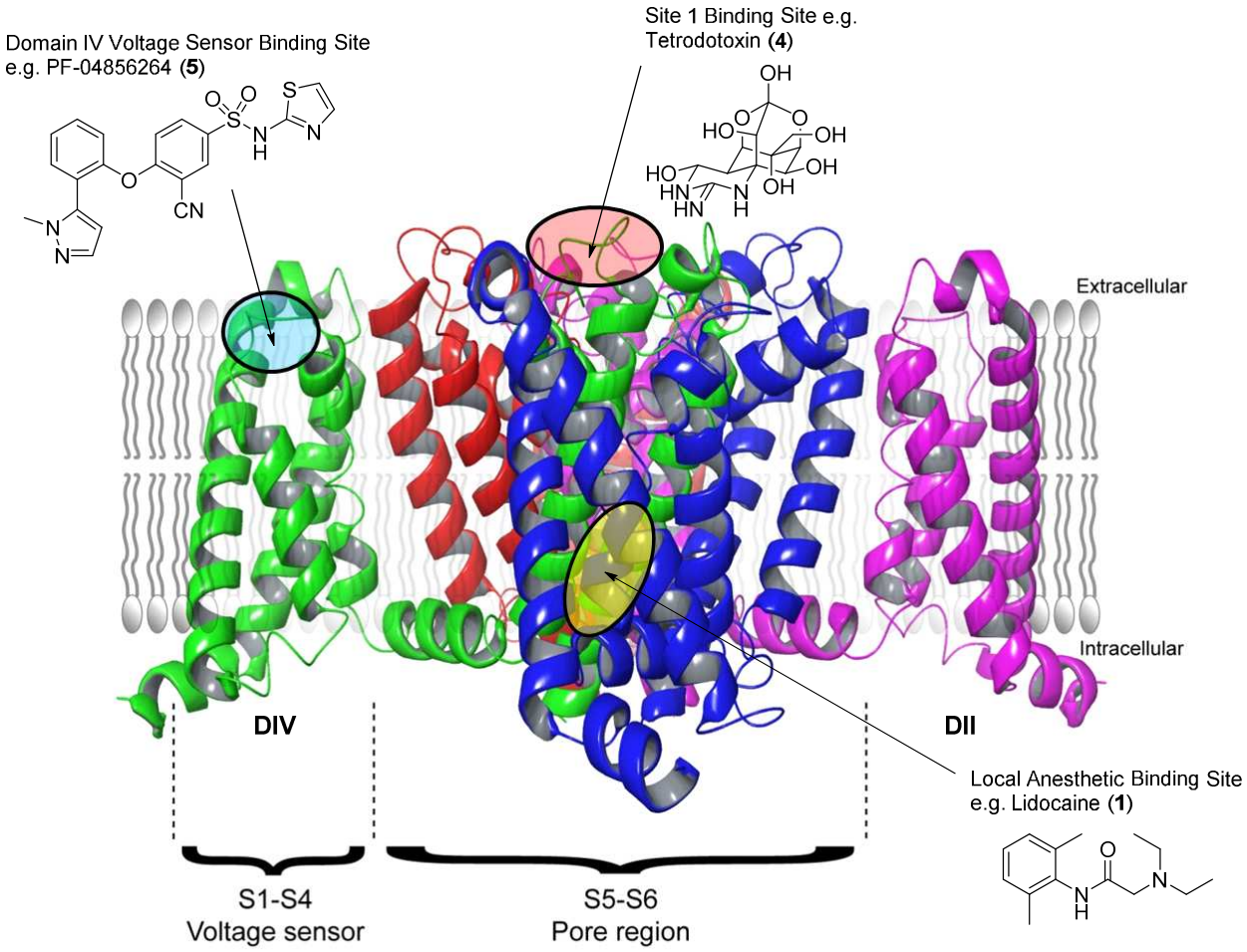

Figure 2. Transmembrane view of sodium channel from the bacterium *Arcobacter butzleri* (Na_VAb PDB code 3RVY)[11] Domains DI-DIV are represented in different colors (DI – red, DII – magenta, DIII – blue, DIV – green). The postulated binding sites are highlighted for local anesthetics (yellow), tetrodotoxin (red) and acidic aryl sulfonamides (blue).

Many groups have subsequently actively targeted this novel binding site which offers enhanced sub-type selectivity over traditional non-selective pore region binding ligands.[12] However, this

has presented many medicinal chemistry and development challenges associated with progression of high molecular weight, lipophilic, acidic small molecules.

Herein we report the work that resulted in the discovery and optimization of a series of acidic diaryl ether aryl sulphonamides leading to the delivery of a clinical candidate with enhanced sub-type selectivity vs known agents.

RESULTS AND DISCUSSION

Initial work focused on replacement of the 2-amino thiazole moiety from early leads such as compound **5** to mitigate the risk of idiosyncratic drug toxicity. The risk associated with a 2-amino thiazole group is exemplified by Sudoxicam (**6**) which was removed from Phase III clinical trials due to hepatotoxicity. Its suspension has been attributed to cytochrome P450 mediated ring oxidation to an electrophilic epoxide **7** (Figure 3).[13] Subsequent hydrolytic ring scission yields acylthiourea metabolite **8** capable of oxidizing glutathione and proteins. Therefore, we sought suitable replacements for this known structural alert whereby the 2-sulfonamido linked thiazoles **9** had the potential to undergo a similar metabolic fate as **6** to reveal both reactive epoxide intermediates **10** and potentially hepatotoxic sulfonylthiourea adducts **11**.

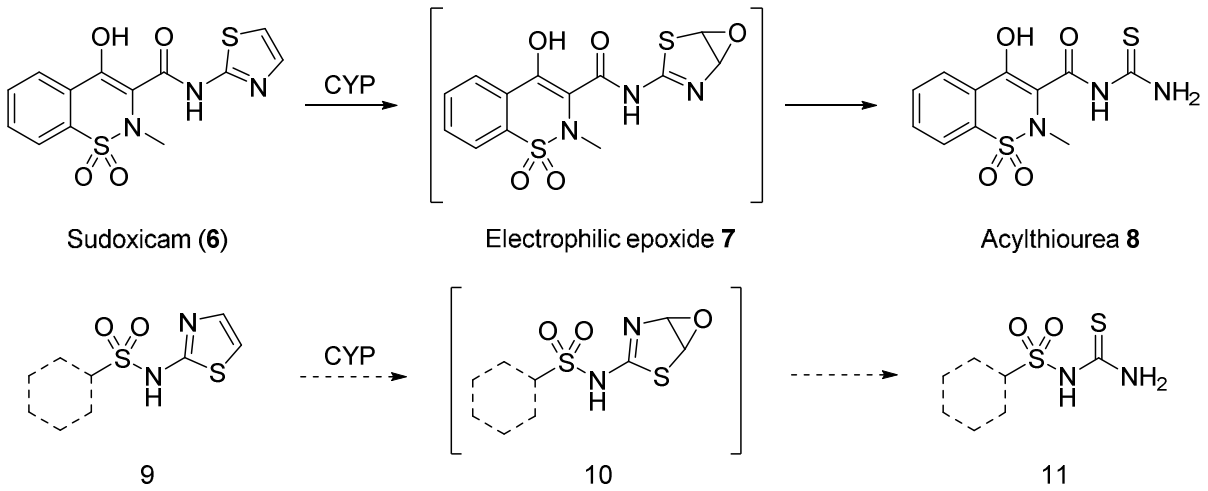

Figure 3. Metabolic pathway of hepatotoxin Sudoxicam (**6**) and implication for acidic 2-amino thiazole containing aryl sulfonamide $Na_V1.7$ series.

Replacement of the 2-aminothiazole with a number of other 5 and 6 membered heterocycles (**12-20**) was successful in maintaining good to excellent levels of $hNa_V1.7$ activity whilst maintaining high levels of $Na_V1.5$ selectivity (Table 1). Furthermore, these alternative hetrerocycles eliminated the potential for thiourea adducts formation resulting from cytochrome P450 (CYP) mediated ring oxidation. Incorporation of an additional nitrogen atom into the thiazole ring provided more acidic 1,2,4-thiadiazole analogues **12-14** (pka's ~3.5) and 1,3,4-thiadiazole regioisomers **15-16** (pka's ~4.5) which demonstrated high lipophilic efficiency (LipE) and selectivity over $hNa_V1.5$.

Table 1. Selected SAR of core substitution and heterocyclic RHS[a]

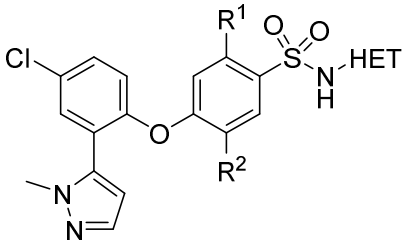

	R^1, R^2	HET	clogD[b]	$hNa_V1.7$ IC_{50} (nM)[c]	$hNa_V1.5$ IC_{50} (nM)[c]	HLM CL_{int}, app (µL/min/mg)	CYP3A4 IC_{50} (nM)	CYP2C9 IC_{50} (nM)	LipE[d]
12	H, CN	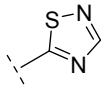	0.9	21	>30000	92	556	517	6.8
13	H, F	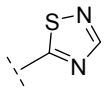	1.2	31	15060	>262	N.D.	N.D.	6.3
14	F, F	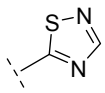	1.2	5	22210	>320	<30	39	7.1

15	H, CN	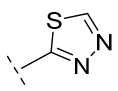	0.5	244	25448	68	N.D.	N.D.	6.1
16	F, Cl	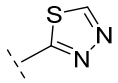	1.2	20	>30000	>300	11068	100	6.5
17	H, CN	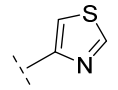	1.8	465	>10000	65	>30000	1368	4.5
18	F, Cl	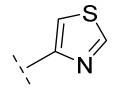	2.2	34	25786	229	26588	37	5.3
19	F, Cl	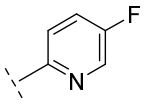	2.9	57	>10000	>320	N.D.	N.D.	4.3
20	F, Cl	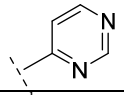	1.5	30	>10000	90	1058	184	6.0

[a]N.D. = not determined. [b]clogD calculated logD based on shake-flask method in octanol and water at $pH_{7.4}$. [c]V_{half} inactivation protocol using PatchXpress™ platform (mean IC_{50} >2 replicates).[14] [d]LipE=-logIC_{50}-clogD.

Interestingly the 4-thiazole analogue in combination with a nitrile core **17** lost significant LipE although this could be regained by core substituent replacement to the more lipophilic F/Cl analogue **18**. Pleasingly 6-membered heterocyclic replacements such as fluoro-pyridyl **19** and pyrimidyl **20** were also tolerated in combination with F/Cl core substituents although were not as efficient as their thiadiazole counterparts. However, all these molecules suffered from high human liver microsome (HLM) clearance with N-demethylation of the LHS pyrazole group confirmed as the major metabolite in metabolite identification studies. Furthermore, we were concerned by significant inhibition of the CYP isoforms 3A4 and 2C9.

Table 2. Broader Na_V pharmacology profile for compounds **12** and **13**.[a]

	12	**13**
hNa_V1.1 IC_{50} (nM)	>3000	216

$hNa_V1.2$ IC_{50} (nM)	276	149
$hNa_V1.3$ IC_{50} (nM)	>3000	292
$hNa_V1.5$ IC_{50} (nM)	>30000	15060
$hNa_V1.6$ IC_{50} (nM)	199	510
$hNa_V1.7$ IC_{50} (nM)	21	31
$hNa_V1.8$ IC_{50} (nM)	>10000	>3000
$rNa_V1.7$ IC_{50} (nM)	813	124

[a] V_{half} inactivation protocols using PatchXpress™ platform.[14]

Intriguingly, core substitution changes at R^2 imparted a dramatic effect on the sub-type and orthologue selectivity as demonstrated by a broader Na_V pharmacology profiling of matched pairs **12** and **13** (Table 2). With the exception of $hNa_V1.6$ the selectivity window for nitrile core analogue **12** was superior to its fluoro partner **13**, particularly $hNa_V1.1$ (>140x vs 7x respectively) and $hNa_V1.3$ (>140x vs 9x respectively). Furthermore, a shift in the rat $Na_V1.7$ activity was noted (39x vs 4x for compounds **12** and **13** respectively) which remained a key consideration in selecting molecules for in vivo evaluation throughout the drug discovery campaign. The excellent LipE and Na_V sub-type selectivity profile of the 1,2,4-thiadiazole in combination with a nitrile R^2 substituent (as represented by compound **12**) became the focus and we turned our attention to solving the HLM and CYP inhibition liabilities through modifications to the pendant ortho-substituted heterocycle (Table 3).

Table 3. Selected SAR of ortho-substituted phenyl substitution

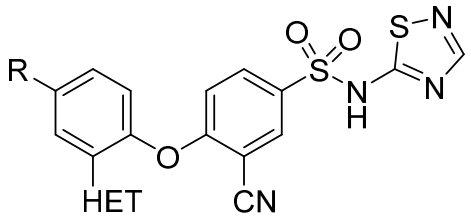

	R	HET	logD[a]	$hNa_V1.7$ IC_{50} (nM)[b]	$hNa_V1.5$ IC_{50} (nM)[b]	HLM CL_{int}, app (µL/min/mg)	CYP3A4 IC_{50} (nM)	CYP2C9 IC_{50} (nM)	LipE[c]
21	Cl	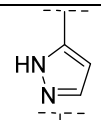	1.6	30	25231	22	400	205	5.9
22	Cl	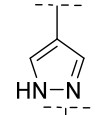	1.7	4	17060	17	505	83	6.7
23	CF_3	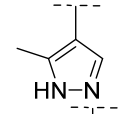	2.0	2	11102	28	737	372	6.7
24	Cl	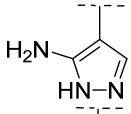	1.0	11	>10000	<8	827	894	7.0
25	Cl	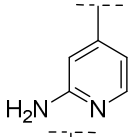	1.6	9	>10000	39	205	279	6.4
26	CF_3	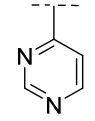	0.9	325	25578	39	910	180	5.6
27	CF_3	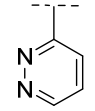	0.7	324	43699	19	616	321	5.8
28	CF_3	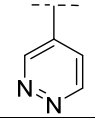	0.7	13	35118	14	1271	2200	7.2

[a]logD measured via shake-flask method in octanol and water at $pH_{7.4}$. [b]V_{half} inactivation protocol using PatchXpress™ platform.[14] [c]LipE=-logIC_{50}-logD.

Des-methyl analogue **21** significantly increased metabolic stability in HLM compared to parent molecule **12** whilst symmetrical pyrazole derivative **22** further increased LipE in combination with low HLM. However, both analogues continued to suffer from high CYP2C9 inhibition (7x and 20x for compounds **21** and **22** respectively) giving the potential for a significant drug-drug

interaction (DDI). To aid design of molecules with reduced CYP2C9 inhibition liability we extended our studies to explore co-crystallization of our $Na_V1.7$ aryl sulfonamides in CYP2C9. Pleasingly, we were able to solve a crystal structure of a related 2-aminothiazole analogue **29** in complex with CYP2C9 (Figure 4). Critically, the RHS acidic moiety interacts with a key Arg108 residue orientating the LHS of the ligand towards the heme region. In this case the pyrazole forms T-stacking and N-donor interactions with the iron complex. Given the RHS acidic heterocyclic sulfonamide group was a crucial pharmacophore for $Na_V1.7$ inhibition our strategy to decrease CYP2C9 inhibition was to disrupt the hemo interaction through steric and/or electronic modifications to the pendent LHS heterocycle.

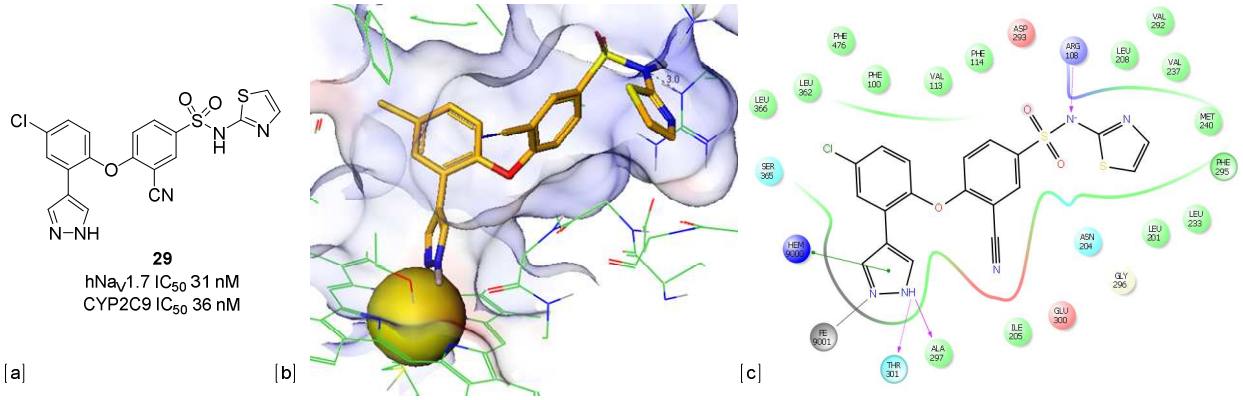

Figure 4. (a) Structure and profile of 2-aminothiazole analogue **29**. (b) X-ray crystal structure of **29** in complex with CYP2C9 (PDB code 5K7K). Iron atom shown as a yellow sphere. (c) Key interactions between **29** and CYP2C9. Pink arrows indicate H-bond interactions with the protein (dotted lines indicate interactions with sidechains and filled lines indicate interactions with the backbone). Green arrows indicate stacking interactions while brown arrows indicate other contacts (in this case, the interaction with Fe^{2+}). Residues are colored by type: red are acidic residues; green are hydrophobic residues; cyan are polar residues and blue are basic residues.

Based on this hypothesis, substitution of the pyrazole group with either a methyl or amino group provided potent, selective and high LipE ligands **23** and **24** respectively. Both compounds also demonstrated a significant improvement in CYP2C9 selectivity (186x and 81x for compounds **23** and **24** respectively) likely due to unfavorable interactions with the protein. Conversely, six-membered heterocycles proved more challenging replacements to boost the CYP2C9 selectivity window. Amino-pyridine **25** showed no improvement in CYP selectivity and diazole analogues such as pyrimidine **26** and pyridazine **27** eroded $Na_V1.7$ activities with concomitant shift in LipE independent from CYP2C9 activity resulting in no selectivity. However, symmetrical pyridazine analogue **28** provided an excellent balance of primary activity, sub-type selectivity and lipophilicity in combination with reduced CYP liability (169x for 2C9 and 98x for 3A4) in one of the most efficient molecules synthesized on the project (LipE = 7.2). The significant reduction in CYP2C9 inhibition for pyridazine **28** was not expected and is a clear outlier from related unsubstituted 6-membered heterocyclic ring systems. We hypothesized that the unusual adjacent dual lone pair system of the pyridazine nitrogens form unfavorable interactions with the heme region of CYP2C9. Unfortunately, attempts to better understand these interactions via co-crystallization of pyridazine containing analogues in CYP2C9 failed.

Several lead compounds possessing the 1,2,4-thiadiazole RHS with high LipE (>6.5) and low intrinsic clearance (<30 μL/min/mg) in pre-clinical species were evaluated in pharmacokinetic (PK) studies (Table 4). Following intravenous (IV) dosing of pyrazole derivatives **22** and **23** in rats and dogs much higher plasma clearances were observed compared to their corresponding scaled in vitro microsomal Cl_{int} measurements suggesting a significant contribution from non-metabolic clearance pathway(s). Oral dosing in rat for compound **23** and dog for compound **22** also demonstrated low bioavailability consistent with a contribution from incomplete absorption

which we attributed, based on data from the RRCK assay, to low passive permeability for these high TPSA, acidic (pKa ~3.5) molecules. Despite its reduced lipophilicity, pyridazine analogue **28** also showed very high clearance in rat and moderate clearance in dog. Following IV administration of **28** to bile duct cannulated rats ~73% of the dose was excreted in bile as unchanged drug during the 6 hour study suggesting the high clearance was non-metabolic. Early PK work with this chemotype also confirmed our hypothesis that molecules in this physicochemical space (high MW, high TPSA, acids) demonstrate very low levels of CNS exposure. Given $Na_V1.7$ is highly expressed in peripheral sensory neurons we rationalized only peripheral block of $Na_V1.7$ was required for efficacy and that limiting CNS penetration would be desirable to further reduce centrally mediated toxicity effects (e.g. via inhibition of $Na_V1.1$ and $Na_V1.2$).

Table 4. Physicochemical, in vitro ADME and pre-clinical pharmacokinetic profiles for lead 1,3,4-thiadiazoles.[a]

Compound	**22**	**23**	**28**
Physicochemical properties			
MW (Da)	458	506	504
clogP	2.8	3.2	2.2
$logD_{7.4}$	1.7	2.0	0.7
TPSA $(Å)^2$	134	134	131
Solubility at pH6.5 (μM)	259	>300	>300

ADME in vitro profile						
RRCK ($x10^{-6}$ cm/sec)	2.1		1.1		0.7	
HLM/RLM/DLM, Clint (μL/min/mg)	17 / 26 / <5		28 / 29 / 9		14 / 23 / <5	
Hhep, Rheps, DHeps Clint (μL/min/10^6 cells)	18 / 5 / N.D.		34 / N.D./N.D.		7 / 11 / N.D.	
hPPB, rPPB, dPPB (Fu)	<0.001, 0.0022, 0.0022		0.0015, 0.0043, 0.0039		0.00543, 0.015, 0.021	
in vivo PK	Rat	Dog	Rat	Dog	Rat	Dog
IV dose (mg/kg)	1	0.1	1	0.1	1	0.1
Cl_p (mL/min/kg)	43	6.5	40.1	21.2	58.0	10.0
Cl_u (mL/min/kg)	19545	2955	9325	5435	3866	476
V_{ss} (L/kg)	2.3	0.5	6.3	1.8	1.3	1.2
$T_{1/2}$ (h)	<1	0.9	5.1	1.2	0.2	3.1
Oral dose (mg/kg)	N.D.	0.13	3	N.D.	3	N.D.
C_{max} (ng/mL)		18	4		1	
$AUC_{0\rightarrow\infty}$ (ng*h/mL)		40	26		5	
F (%)		23	<5		<1	

[a]N.D. = not determined.

Several LHS substituents had now been identified which were optimized for LipE, metabolic stability and CYP2C9 selectivity. Subsequent designs to re-explore the core substituents and alternative heterocyclic RHS groups were initiated in an attempt to reduce the TPSA and acidity

and explore the impact on pre-clinical clearance and oral absorption. Furthermore, earlier evidence (as observed with representatives in Table 1) also suggested alternative non-1,2,4-thiadiazole heterocycles could offer improvements in the selectivity over CYP3A4 inhibition, reducing any associated DDI risk.

Utilizing pyridazine **28** as an advanced lead the nitrile core was switched to the lower TPSA expressing F/Cl substitution pattern and less acidic RHS heterocyclic alternatives were synthesized (Table 5). 1,3,4-Thiadiazole derivative **30** (measured pKa 4.0) maintained high LipE and improved HLM Cl_{int} and CYP3A4 selectivity (536x) over compound **28**. The 4-thiazole derivative **31** (estimated pKa 5.6) also showed reduced CYP3A4 liability although this more lipophilic expression showed moderate turnover in HLM and reduced LipE.

Table 5. Heterocyclic changes with an optimized pyridazyl LHS

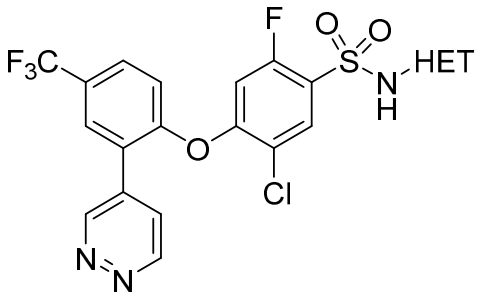

	HET	logD[a]	TPSA	$hNa_V1.7$ IC_{50} (nM)[b]	$hNa_V1.5$ IC_{50} (nM)[b]	HLM $CL_{int,app}$ (µL/min/mg)	CYP3A4 IC_{50} (nM)	CYP2C9 IC_{50} (nM)	LipE[c]
30	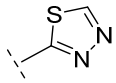	0.8	107	21	>30000	<8	>11248	1101	6.9
31	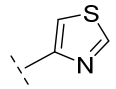	1.6	94	26	22451	17	>30000	1365	6.0

[a]logD measured via shake-flask method in octanol and water at $pH_{7.4}$. [b]V_{half} inactivation protocol using PatchXpress™ platform.[14]
[c]LipE=-logIC_{50}-logD.

The high LipE and improved CYP2C9 profile for amino-pyrazole example **24** (Table 3) was intriguing although the high TPSA and HBD/HBA expression of this LHS moiety led to significant concerns over oral absorption. However, an exploration of alternative RHS expressions with the lower TPSA expressing F/Cl core was undertaken providing 1,3,4-thiadiazole and 4-thiazole derivatives **32-34**, all showing an improved CYP3A4 selectivity window whilst maintaining good levels of $Na_V1.7$ activity (Table 6). Unfortunately, following a 3 mg/kg oral administration of high LipE thiadiazole **32** in rat, oral bioavailability was calculated to be <5 % (despite clearance approximately 25% liver blood flow) suggesting poor absorption with this high TPSA, moderately acidic (measured acidic pKa 4.3) example. However, the lower TPSA and weakly acidic 4-thiazole derivatives **33** and **34** (measured acidic pKa 6.3) both demonstrated good oral bioavailability in rat and a PK summary for compound **34** is provided in table 8 and will be discussed in more detail later in this manuscript.

Table 6. Heterocyclic changes with an optimized amino-pyrazole LHS

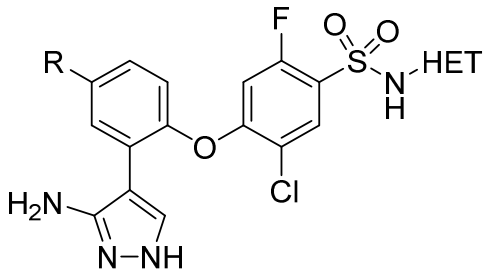

	R	HET	logD[a]	TPSA	$hNa_V1.7$ IC_{50} (nM)[b]	$hNa_V1.5$ IC_{50} (nM)[b]	HLM CL_{int}, app (µL/min/mg)	CYP3A4 IC_{50} (nM)	CYP2C9 IC_{50} (nM)	LipE[c]
32	CF_3	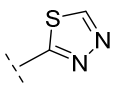	0.9	136	8	14413	<9	>30000	658	7.2
33	CF_3	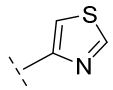	2.2	123	9	10549	<9	>30000	552	5.8

34	Cl	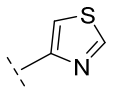	2.3	123	11	>10000	10	>30000	299	5.5

[a]logD measured via shake-flask method in octanol and water at $pH_{7.4}$. [b]V_{half} inactivation protocol using PatchXpress™ platform.[14] [c]LipE=-logIC_{50}-logD.

During the course of our SAR studies we identified that zwitterionic ligands (via incorporation of a basic center distal to the key acidic pharmacophore) were also well tolerated as hNa_V1.7 inhibitors. Alkylated azetidine substituted pyrazoles **35-38** provided molecules with good levels of Na_V1.7 activity and excellent selectivity against Na_V1.5 (Table 7). Unfortunately PK profiling of 1,2,4-thiadiazole analogue **35** resulted in liver blood flow clearance in rat thwarting any desire to progress further. Pleasingly, 4-thiazole analogues **36-38** provided higher selectivity windows over CYP inhibition. Furthermore, increasing the size of the R^3 alkyl group from a methyl in example **37** to ethyl analogue **38** was not detrimental to Na_V1.7 activity or metabolic stability in HLM and continued to widen the CYP inhibition window. Interesting, despite its lower LipE, nitrile core example **36** showed impressive levels of Na_V sub-type selectivity (see table 8 for full pharmacology profile) consistent with earlier observations for the 1,3,4-thiadiazole, nitrile core acidic molecules.

Table 7. Optimization of zwitterionic substrate

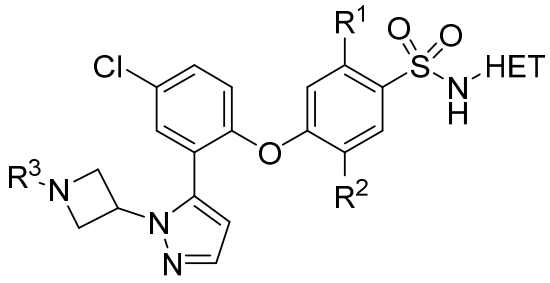

R^1, R^2	R^3	HET	logD[a]	TPSA	hNa_V1.7 IC_{50} (nM)[b]	hNa_V1.5 IC_{50} (nM)[b]	HLM CL_{int}, app (µL/min/ mg)	CYP3A4 IC_{50} (nM)	CYP2C9 IC_{50} (nM)	LipE[c]

35	F, F	Me	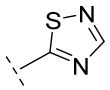	1.0	102	3	29291	N.D.	427	264	7.5
36	H, CN	Et	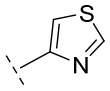	1.4	113	46	>30000	13	12239	17992	5.9
37	F, F	Me	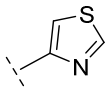	1.3	89	7	>30000	27	15124	1012	6.8
38	F, F	Et	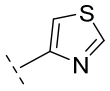	1.6	89	10	>10000	25	>30000	3234	6.4

[a]logD measured via shake-flask method in octanol and water at $pH_{7.4}$. [b]V_{half} inactivation protocol using PatchXpress™ platform.[14]
[c]LipE=-logIC_{50}-logD.

More extensive analysis of three advanced molecules (examples **30**, **34** and **36**) with superior in vitro ADME and primary pharmacology profiles was carried out (Table 8). Upon full Na_V pharmacology profiling excellent sub-type selectivities were confirmed together with a general shift in the orthologue activity which was most pronounced in rat. Compounds **30**, **34** and **36** were also tested for off-target pharmacology against a broad range of receptors, enzymes and ion channels at CEREP (Bioprint) and within Pfizer (see SI). Encouragingly, a low perceived safety risk was posed by the levels of activity observed in these selectivity panels.

Generally within the series the preclinical in vivo PK was not reliably predicted by in vitro metabolic Cl_{lint} using appropriate liver microsomes or hepatocyte systems. It was also notable that there were distinct trends in PK between species with rats typically displaying high clearance and atypical PK profiles for acidic molecules, such as high $V_{ss,}$ while dogs typically showed lower clearance and more typical PK.[15] Various pieces of in vitro data, including Sandwich Cultured Human Hepatocytes (data not shown) and OATP expressing cell lines, suggested a potential contribution to clearance from active hepatic uptake. It was also noted in bile duct cannulated rat studies that these compounds showed significant contributions from

biliary clearance of unchanged drug, although the relevance to other species was not well understood.

The failure of in vitro scaling to predict preclinical PK, inconsistent preclinical PK between species, and data suggesting the potential for a significant contribution from non-metabolic clearance routes, raised significant concerns of the likely accuracy of human PK predictions for compounds in this series. Therefore, these three compounds from the diaryl ether aryl sulfonamides series described, **30**, **34** and **36**, were chosen for inclusion in a human microdose study, where the PK profiles were determined following intravenous and oral administration.[16] A fourth compound from an alternative indazole series was also included in the microdose study and will be the topic of future disclosures. It is noteworthy that whilst LipE proved a key parameter in ligand design to improve overall physicochemical properties for the series, compounds **34** and **36** display some of the lowest LipEs reported for our most advanced inhibitors. This is a reflection of the major challenges faced with this chemotype to deliver structurally differentiated molecules for a human microdose study balancing low DDI risk, high oral absorption and acceptable pre-clinical clearance.

Table 8. Physicochemical properties, in vitro ADME, Na_V pharmacology and pre-clinical pharmacokinetic profiles for lead microdose molecules.[a]

Compound	**30**	**34**	**36**
Physicochemical properties			
MW (Da)	532	500	541
clogP	3.1	4.2	4.4
$logD_{7.4}$	0.9	2.6	1.4
pK_a acid, [base]	4.3	6.3	6.5 [7.4]

TPSA (Å)^2	107		123		113	
Solubility at pH6.5 (μM)	286		<0.3		>262	
ADME in vitro profile						
RRCK (x10^{-6} cm/sec)	0.7		3.8		3.2	
MDCK-MDR1 P_{app} AB/BA (x10^{-6} cm/sec)	<0.5/1.1		0.7/6.3		<0.5/11	
HLM/RLM/DLM, Cl_{int} (μL/min/mg)	<8 / <17 / <5		<10 / <18 / <8		<20 / 41 / 23	
Hhep, Rheps, DHeps Cl_{int} (μL/min/10^6 cells)	<8 / 8 / N.D.		15 / <5 / N. D.		7 / <5 / N.D.	
hPPB, rPPB, dPPB (Fu)	0.0016, 0.0221, 0.0055		0.0015, 0.0134, 0.0075		0.0648, 0.125, 0.231	
OATP1B1 (transfected/wild type)	N.D.		N.D.		2.05	
OATP1B3 (transfected/wild type)	N.D.		N.D.		2.13	
OATP2B1 (transfected/wild type)	N.D.		N.D.		1.83	
Na_V pharmacology[b]						
hNa_V1.1 IC_{50} (nM)	8750		677		>10000	
hNa_V1.2 IC_{50} (nM)	398		119		2044	
hNa_V1.3 IC_{50} (nM)	>10000		>10000		>10000	
hNa_V1.4 IC_{50} (nM)	>30000		>10000		>10000	
hNa_V1.5 IC_{50} (nM)	>30000		>10000		>30000	
hNa_V1.6 IC_{50} (nM)	1109		173		1636	
hNa_V1.7 IC_{50} (nM)	21		15		46	
hNa_V1.8 IC_{50} (nM)	>30000		>10000		>10000	
rNa_V1.7 IC_{50} (nM)	5450		153		3140	
dNa_V1.7 IC_{50} (nM)	132		16		263	
in vivo PK	Rat	Dog	Rat	Dog	Rat	Dog
IV dose (mg/kg)	1	0.1	1	0.1	1	0.1
Cl_p (mL/min/kg)	40.3	2.0	6.0	2.7	>70	15
Cl_u (mL/min/kg)	1824	364	448	360	>560	65

V_{ss} (L/kg)	11.0	0.5	1.3	0.2	29.7	0.9
$T_{1/2}$ (h)	6.6	4.6	4.4	4.0	2.2	1.1
Oral dose (mg/kg)	3	3	3	3	3	N.D.
T_{max} (h)	1.5	1.5	2.0	0.9	0.3	
C_{max} (ng/mL)	73.2	2890	541	998	92.7	
F (%)	16	54	27	35	68	

[a]N.D. = not determined. [b]V_{half} inactivation protocols using PatchXpress™ platform.[14]

The data from the human microdose study are summarized in Table 9 and Figure 5. Compound **36** was ruled out based on its short plasma half-life as the peak to trough ratios, based on twice-daily administration, would have required a high therapeutic index. Compounds **30** and **34** exhibited half-life values that would support twice-daily oral administration. However, on the basis of superior $Na_V1.7$ potency and a PBPK modelling prediction suggesting the clinical target concentration of 3x IC_{50} unbound plasma concentration at trough would be obtained at a lower dose, it was decided to progress compound **34** to further clinical trials. It was subsequently shown to be safe and well-tolerated up to a single oral dose of 2400 mg, providing significant coverage of the $Na_V1.7$ IC_{50} (C_{max} free plasma concentration of 226 nM providing ~20x $Na_V1.7$ IC_{50} at the 2400 mg dose).

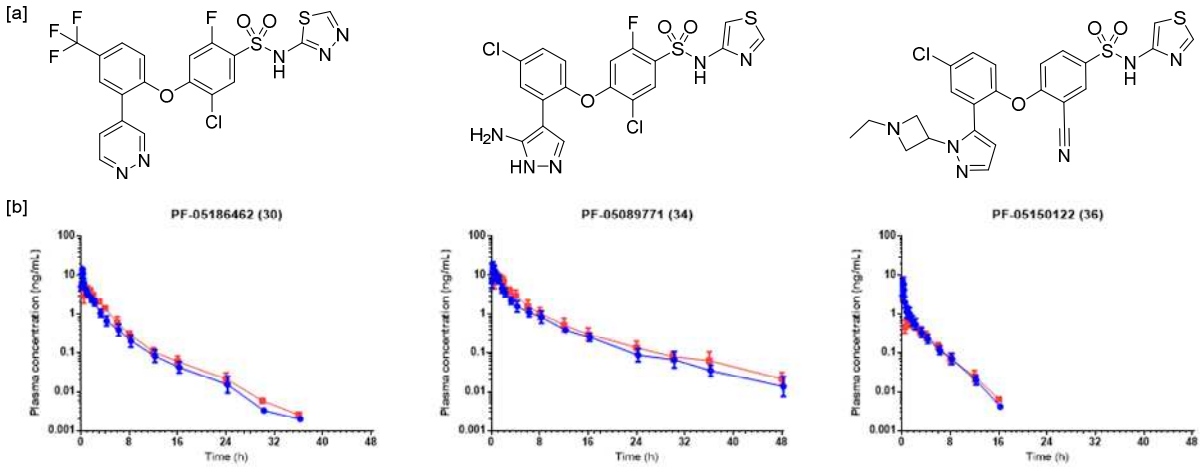

Figure 5. (a) Structures of **30** (PF-05186462[8]), **34** (PF-05089771[8]) and **36** (PF-05150122[8]). (b) Human mean plasma concentrations following 100 µg intravenous (blue) and 100 µg oral microdoses (red).

Table 9. Human pharmacokinetic microdose data for **30**, **34** and **36**.

Compound	**30**	**34**	**36**
IV dose (µg)	100	100	100
Cl_p (mL/min/kg)	1.2	0.5	3.6
Cl_u (mL/min/kg)	745	350	55
V_{ss} (L/kg)	0.18	0.15	0.41
$T_{1/2}$ (h)	4.5	6.5	2.2
Oral dose (µg)	100	100	100
C_{max} (ng/mL)	4.8	11	0.67
F (%)	101	110	52

Significant in vitro and in vivo profiling of aryl sulfonamide **34** and close structural analogue **33** has been reported in an earlier manuscript.[17] Detailed manual electrophysiology characterization confirm **34** is a state-dependent and selective inhibitor of $Na_V1.7$. Inhibitory effects of

compound **34** on action potentials in spinal slice electrophysiology recordings, mouse and human DRG neurons, in addition to in vivo efficacy of **33** in a mouse capsaicin-induced neurogenic flare model, further demonstrate the multiple contributions of $Na_V1.7$ in nociceptor signaling.[17]

SYNTHETIC CHEMISTRY

The key compounds **30**, **34**, **36** were prepared by S_NAr reaction, joining a heteroaryl phenol left hand side (LHS) with a suitably protected heteroaryl sulfonamide right hand side (RHS) via an ether linkage.

Scheme 1. Synthesis of Compound **34**[a]

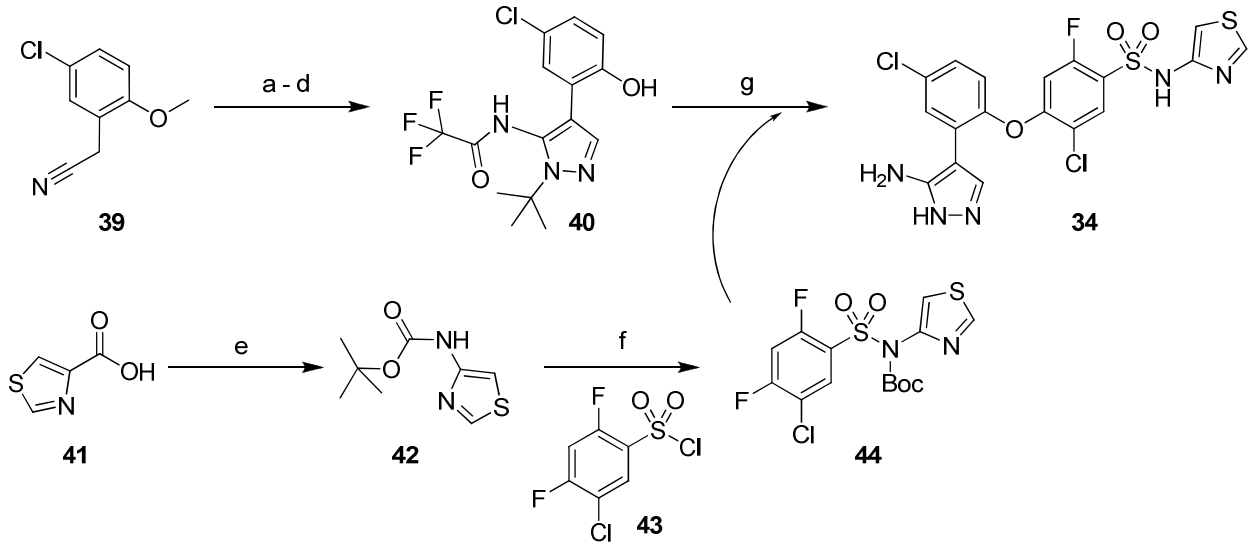

[a]Reagents and conditions. (a) CH_3CH_2OCHO, sodium, reflux, 16 h (b) $(CH_3)_3CHNHNH_2.HCl$, EtOH, reflux 24 h (c) $(CF_3CO)_2O$, Et_3N, CH_2Cl_2, 16 h (d) BBr_3, CH_2Cl_2, 0 °C, 45 min, 66% over 4 steps (e) diphenylphosphoryl azide, t-BuOH, Et_3N, reflux, 18 h, 77% (f) LiHMDS, THF, 0 °C, 30 min, 50% (g) i) NaH, DMF, ii) K_2CO_3, 55 °C, 3 days iii) Na_2CO_3 (aq), CH_3OH, 55 °C 16 h, iv) HCl, CH_3OH, 50 °C, 16 h 12% over 4 steps.

For the synthesis of compound **34** (Scheme 1) the LHS was constructed in one pot by standard aminopyrazole ring formation utilizing 2-(5-chloro-2-methoxyphenyl)acetonitrile **39**, ethyl formate and t-butyl hydrazine hydrochloride followed by trifluoroacetate amine protection.

Finally boron tribromide demethylation yielded the desired phenol **40**. The protected heteroaryl sulfonamide RHS was prepared by reaction of tert-butyl thiazol-4-ylcarbamate **42** (made via Curtuis rearrangement of the corresponding thiazole carboxylic acid **41**) with aryl sulfonyl chloride **43** to generate the protected RHS **44**. Base promoted S_NAr between the LHS and RHS, and subsequent protecting group removal yielded the desired final product **34**.

Scheme 2. Synthesis of Compound **30**[a]

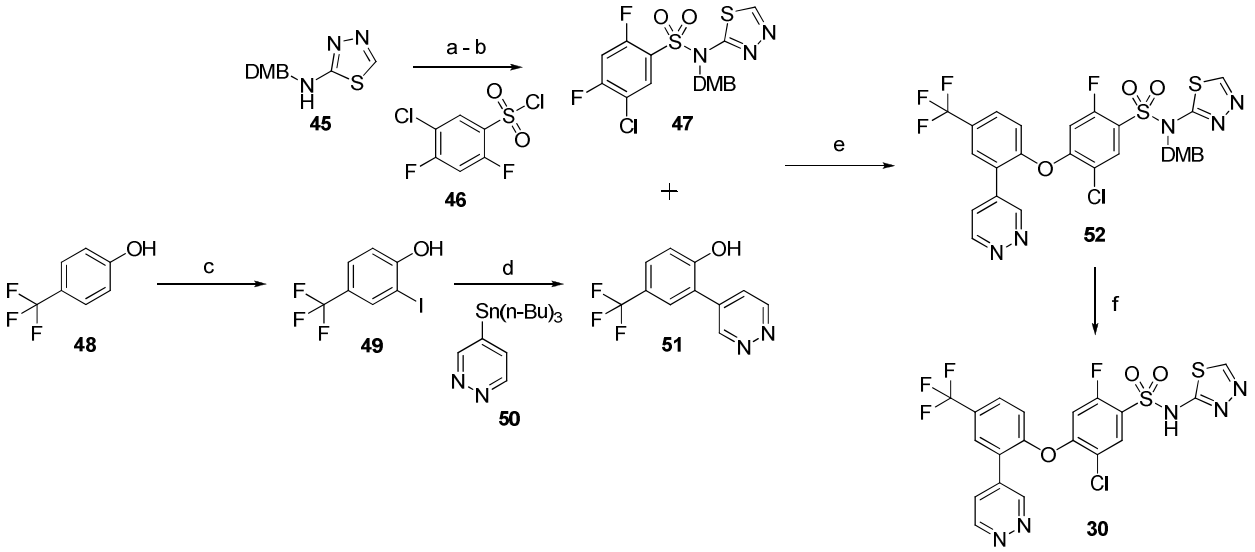

[a]Reagents and conditions: (a) LiHMDS, 2-Me-THF, -45 °C, 45 min.; (b) Compound **46,** -45 °C to 0 °C, 2 h, 78%; (c) Iodine, Na_2CO_3, THF/Water, 24 h, 41 %; (d) CH_3CN, CuI, $(PPh_3)_4$, CsF, 50 °C, 2 h, 68%; (e) K_2CO_3, DMSO, 16 h, 67%; (f) 4M HCl / dioxane, 3 h, 82%

Synthesis of compound **30** (Scheme 2) was initiated by aryl sulfonyl chloride **46** addition to 2,4-dimethoxybenzyl (DMB) protected aminothiadiazole **45** to build the RHS for this scaffold. Construction of the LHS was achieved by iodination of 4-trifluoromethyl phenol **48** to yield compound **49** followed by copper mediated addition of 4-(tributylstannyl) pyridazine **50** to construct diaryl phenol **51**. Finally base mediated S_NAr and HCl cleavage of the DMB protecting group gave compound **30**.

Scheme 3. Synthesis of Compound **36**[a]

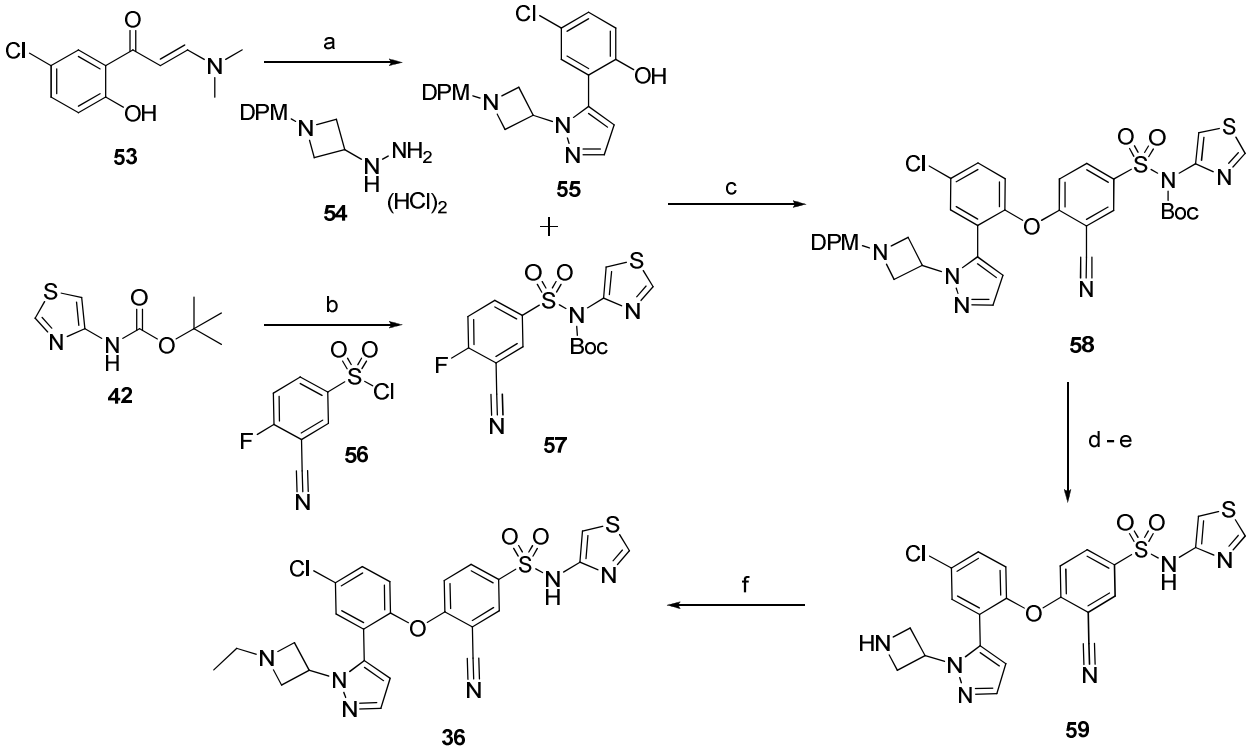

[a]Reagents and Conditions (a) Compounds **53** and **54** (see SI for synthesis), EtOH, 0 °C, 2 h, 42%; (b) LiHMDS, -78 °C to room temp., 16 h, 54%; (c) K_2CO_3, DMSO, room temp. 4 h, 24%; (d) i) Chlororethyl chloroformate, proton sponge, CH_2Cl_2, room temp. 3.5 h. ii) CH_3OH, reflux, 4 h; (e) 4M HCl/dioxane, 2 h, 33% over 3 steps; (f) Sodium triacetoxyborohydride, CH_2Cl_2/CH_3OH, Et_3N, 0 °C, acetaldehyde, 1.5 h, 60%.

In an analogous manner the LHS of compound **36** (Scheme 3) was prepared by standard condensation of enamine **53** with diphenylmethyl (DPM) protected azetidinyl-hydrazine hydrochloride **54** to generate the required phenol **55.** The RHS **57** was prepared analogously to that in Scheme 1 and subsequent S_NAr provided fully protected **58**. DPM removal via treatment with proton sponge and chloroethyl chloroformate followed by complete Boc removal with HCl gave the desired fully deprotected **59**. Finally, reductive amination with acetaldehyde gave the desired compound **36**.

CONCLUSIONS

In summary, a series of diaryl ether aryl sulfonamides has been identified as potent and highly subtype selective inhibitors of $Na_V1.7$. This high molecular weight, acidic chemotype represented a significant challenge in human pharmacokinetic predictions due to non-metabolic clearance pathways predominating. A human microdose study was therefore carried out on 3 diverse ligands from the series (varying pKa, lipophilicity and chemical diversity) to determine basic PK parameters leading to the nomination of **34** as a clinical candidate. Furthermore, this represents the first potent and selective molecule which binds to the domain IV voltage sensor region of the sodium channel to progress into the clinic. The development of selective agents such as **34** offers new potential therapeutic modalities for acute and chronic pain, which remain a high medical need.

EXPERIMENTAL SECTION

The synthesis of the lead compounds **30**, **34**, **36** are described below. Detailed experimental procedures for the synthesis of all other compounds, their intermediates, and characterization data are provided in the supporting information.

Materials and Methods. Unless otherwise noted, all materials were obtained from commercial suppliers and used without further purification. ^{1}H Nuclear magnetic resonance (NMR) spectra were in all cases consistent with the proposed structures. Characteristic chemical shifts (δ) are given in parts-per-million (ppm) (δ relative to residual solvent peak) using conventional abbreviations for designation of major peaks: *e.g.* s, singlet; d, doublet; t, triplet; m, multiplet; br, broad. The mass spectra (*m/z*) were recorded electrospray ionization (ESI). The following abbreviations have been used for common solvents: $CDCl_3$, deuterochloroform; d_6-DMSO, deuterodimethylsulfoxide; CD_3OD, deuteromethanol. All solvents were reagent grade

and, when necessary, were purified and dried by standard methods. Concentration of solutions after reactions and extractions involved the use of a rotary evaporator operating at a reduced pressure of ca. 20 Torr. Anhydrous solvents were obtained from commercial sources and used as supplied. Organic solvents were dried over anhydrous magnesium sulfate or anhydrous sodium sulfate. All final compounds had a high performance liquid chromatography (HPLC) purity of 95% or greater using one of the methods described in the supporting information.

5-Chloro-2-fluoro-4-[2-pyridazin-4-yl-4-(trifluoromethyl)phenoxy]-N-1,3,4-thiadiazol-2-ylbenzenesulfonamide (30). To a stirred solution of 5-chloro-N-(2,4-dimethoxybenzyl)-2-fluoro-4-[2-pyridazin-4-yl-4-(trifluoromethyl)phenoxy]-N-1,3,4-thiadiazol-2-ylbenzenesulfonamide (**52**) (28.1 g, 41.2 mmol) in 1,4-dioxane (250 mL) at room temperature was added a 4M solution of HCl in 1,4-dioxane (300 mL) dropwise over 30 minutes. The resulting suspension was left to stir at room temperature for 3 hours before concentration in vacuo. The residue was azeotroped with diethyl ether (3 x 300 mL) followed by a diethyl ether trituration (200 mL) to provide crude material as a fawn colored solid. This material was suspended in methanol (200 mL) and filtered through Celite, washed with methanol (400 mL) and the resulting filtrate concentrated in vacuo to give a sand colored solid. This material was suspended in water (100 mL) and treated with concentrated ammonium hydroxide (60 mL) portion wise until pH 9-10 was achieved. The resulting solution was washed with diethyl ether (3 x 75 mL) and the aqueous layer acidified to pH=5 with citric acid. The mixture was then extracted with ethyl acetate (3 x 200 mL) and brine (100 mL) added to aid separation. The combined organic layers were washed with water (200 mL), dried over $MgSO_4$ and concentrated in vacuo to approximately 100 mL whereby a precipitate was observed. This mixture was allowed to stand for 18 hours and the resulting solid filtered and washed with cold ethyl acetate

(10 mL) and dried in vacuo at 60 °C to provide the title compound as a sand colored crystalline solid (17.5 g, 80%). ^{1}H NMR (400 MHz, DMSO-d_6) δ ppm 7.31 (d, *J*=8.60 Hz, 1 H) 7.51 (d, *J*=10.55 Hz, 1 H) 7.87 (dd, *J*=8.99, 2.34 Hz, 1 H) 7.92 - 8.03 (m, 2 H) 8.12 (d, *J*=2.34 Hz, 1 H) 8.83 (s, 1 H) 9.33 (dd, *J*=5.27, 1.37 Hz, 1 H) 9.52 (dd, *J*=2.54, 1.37 Hz, 1 H). HPLC (12min) t_R= 8.35 min, HPLC purity >98%. LCMS (APCI) *m/z* 532 $[M+H]^+$ HRMS (EI) *m/z*: $[M+H]^+$ Calcd for $C_{19}H_{11}ClF_4N_5O_3S_2$ 531.9928, found 531.9919.

4-[2-(5-Amino-1H-pyrazol-4-yl)-4-chlorophenoxy]-5-chloro-2-fluoro-N-1, 3-thiazol-4-ylbenzenesulfonamide (34). To a suspension of sodium hydride (29 mg, 1.2 mmol) in dimethylformamide (1 mL) was added N-(1-tert-butyl-4-(5-chloro-2-hydroxyphenyl)-1H-pyrazol-5-yl)-2,2,2-trifluoroacetamide (**40**) (239 mg, 0.661 mmol) and stirred for 30 minutes. To this was added tert-butyl 5-chloro-2, 4-difluorophenylsulfonyl (thiazol-4-yl) carbamate (**44**) (206 mg, 0.501 mmol) and the reaction stirred for 24 hours. Potassium carbonate (40 mg, 0.3 mmol) was added and the reaction heated at 55 ^{o}C for 3 days. The reaction was cooled, diluted with ethyl acetate (10 mL) and the organic extract washed with water (10 mL) and saturated aqueous sodium chloride solution (10 mL), dried over magnesium sulfate, filtered and concentrated in vacuo. Purification by automated flash column chromatography eluting with ethyl acetate:hexanes (gradient 0:1 to 1:0) afforded intermediate protected product. This residue was dissolved in methanol (1 mL) and sodium carbonate solution (2 M aqueous, 0.08 mL, 0.2 mmol) and water (0.2 mL) added. The reaction was stirred at room temperature for 6 hours and then heated at 55 °C for 16 hours before concentrating in vacuo and purification by flash chromatogray eluting with methanol:dichloromethane (gradient 0:1 to 1:9). The resulting purified material was dissolved in methanol (saturated in gaseous hydrogen chloride) and heated at 50 ^{o}C for 16 hours. Purification by preparative HPLC afforded the title compound HCl salt as

a white solid (31 mg, 12%). ^{1}H NMR - HCl salt (600 MHz, DMSO-d6) δ ppm 6.98 (d, *J*=11.15 Hz, 1 H) 7.10 (d, *J*=1.17 Hz, 1 H) 7.22 (d, *J*=8.80 Hz, 1 H) 7.47 (dd, *J*=8.51, 2.05 Hz, 1 H) 7.73 (br. s., 1 H) 7.90 (d, *J*=7.04 Hz, 1 H) 7.94 (s, 1 H) 8.92 (d, *J*=1.17 Hz, 1 H) ^{1}H NMR - Free base: (600 MHz, DMSO-d6) δ ppm 4.85 (br. s., 2 H) 6.72 (d, *J*=10.56 Hz, 1 H) 7.07 (d, *J*=1.17 Hz, 1 H) 7.21 (d, *J*=8.80 Hz, 1 H) 7.28 - 7.34 (m, 1 H) 7.42 (br. s., 1 H) 7.68 (br. s., 1 H) 7.89 (d, *J*=7.04 Hz, 1 H) 8.90 (d, *J*=1.76 Hz, 1 H) 11.37 (br. s., 1 H) 11.72 (br. s., 1 H), HPLC (12min) t_R= 7.66 min, HPLC purity >98%. LRMS (ESI) m/*z* 501 $[M+H]^+$; HRMS (EI) *m/z*: $[M+H]^+$ Calcd for $C_{18}H_{13}Cl_2FN_5O_3S_2$ 499.9821, found 499.9816.

4-{4-Chloro-2-[1-(1-ethylazetidin-3-yl)-1H-pyrazol-5-yl]phenoxy}-3-cyano-N-1,3-thiazol-4-ylbenzenesulfonamide (36). To a suspension of 4-[2-(1-azetidin-3-yl-1*H*-pyrazol-5-yl)-4-chlorophenoxy]-3-cyano-N-1,3-thiazol-4-ylbenzenesulfonamide, (**59**) (500 mg, 0.797 mmol) in methanol (4 mL) and dichloromethane (4 mL) was added triethylamine (161 mg, 1.59 mmol) and the reaction cooled to 0 °C in an ice/water bath. To the suspension was added sodium triacetoxyborohydride (422 mg, 1.99 mmol) and the reaction was then stirred at 0 °C for 10 minutes. Acetaldehyde (105 mg, 2.39 mmol) was added dropwise and the reaction stirred at 0 °C for 1.5 hours. The solvent was removed *in vacuo* to give an orange oil which was partitioned between dichloromethane (25 mL) and water (25 mL). The organic layer was separated and the aqueous layer was extracted with dichloromethane (2 x 20 mL). The combined organic layers were washed with saturated aqueous sodium chloride solution (20 mL) and filtered through a phase separation cartridge. The solvent was removed in vacuo and the resulting solid was triturated in hot ethyl acetate (10 mL), allowed to cool to room temperature and then filtered to provide the title compound as a white solid (260 mg, 60%). ^{1}H NMR (400 MHz, DMSO-d_6) δ ppm 1.04 - 1.13 (m, 3 H) 3.24 (q, *J*=6.64 Hz, 2 H) 4.16 (br. s., 2 H) 4.42 (br. s., 2 H) 5.11 (br. s.,

1 H) 6.28 (d, *J*=1.95 Hz, 1 H) 6.97 (d, *J*=8.99 Hz, 1 H) 7.09 (d, *J*=1.95 Hz, 1 H) 7.51 (d, *J*=8.60 Hz, 1 H) 7.61 (d, *J*=1.17 Hz, 1 H) 7.68 - 7.75 (m, 2 H) 7.87 (dd, *J*=8.99, 2.34 Hz, 1 H) 8.09 - 8.15 (m, 1 H) 8.90 (d, *J*=2.34 Hz, 1 H) 10.94 (br. s., 1 H). HPLC (12min) t_R= 7.57 min, HPLC purity >98%. LCMS (ESI) *m/z* 541 $[M+H]^+$; HRMS (EI) *m/z*: $[M+H]^+$ Calcd for $C_{24}H_{22}ClN_6O_3S_2$, 541.0883 found 541.0935.

N-[1-*tert*-Butyl-4-(5-chloro-2-hydroxyphenyl)-1H-pyrazol-5-yl]-2,2,2-trifluoroacetamide (40). To a solution of (5-chloro-2-methoxy-phenyl)acetonitrile (**39**) (2.154 g, 11.86 mmol) in ethyl formate (20 mL) was added sodium (605 mg, 26.3 mmol). The reaction was heated at a gentle reflux for 16 hours. After cooling to room temperature, water and dichloromethane were added and the solution adjusted to pH 3 with hydrochloric acid (6 M aqueous solution). The layers were separated and the aqueous layer extracted with dichloromethane (2 x 50 mL). The combined organics were washed with saturated aqueous sodium chloride solution, dried over magnesium sulfate, filtered and evaporated *in vacuo*. Purification by flash column chromatography eluting with ethyl acetate: hexanes (gradient 0:1 to 1:1, by volume) gave a white solid which was dissolved in ethanol (50 mL), *tert*-butylhydrazine hydrochloride (1.77 g, 14.2 mmol) added and solution heated to reflux for 24 hours. The reaction was cooled and evaporated *in vacuo* to give brown oil. This oil was dissolved in dichloromethane (50 mL) and triethylamine (4.2 mL, 30 mmol) and trifluoroacetic anhydride (4.2 mL, 30 mmol) were added. After stirring for 16 hours, the reaction was washed with potassium hydrogen sulfate (1 N aqueous solution), sodium bicarbonate (1 N aqueous solution) and saturated aqueous sodium chloride solution. The organic layer was separated, dried over magnesium sulfate, filtered and concentrated *in vacuo* to give brown oil. This oil was dissolved in dichloromethane (20 mL) and cooled over an ice water bath before the addition of boron tribromide (1 M in dichloromethane,

22 mL, 22 mmol). After stirring for 45 minutes the reaction was added to ice water. The layers were separated and the aqueous layer washed with dichloromethane (2 x 20 mL). The combined organics were dried over magnesium sulfate, filtered and concentrated *in vacuo* to give brown oil. Purification by flash column chromatography eluting with ethyl acetate: hexane (gradient 0:1 to 1:0, by volume) to afford the title compound as a brown oil that solidified to a tan solid upon standing (2.82 g, 66%). ^{1}H NMR (400 MHz, DMSO-d_6) δ ppm 1.56 (s, 9 H) 6.90 (d, *J*=8.58 Hz, 1 H) 7.08 - 7.15 (m, 1 H) 7.17 (d, *J*=2.73 Hz, 1 H) 7.76 (s, 1 H) 9.91 (s, 1 H) 11.38 (s, 1 H). HPLC (6 min), t_R = 3.0 min, HPLC purity >95%. LCMS (ESI) *m/z* 362.4 $[M+H]^+$.

Thiazole-4-yl-carbamic acid *tert*-butyl ester (42). Thiazole-4-carboxylic acid (**41**) (10 g, 77.4 mmol) was slurried in *tert*-butyl alcohol (500 mL). Triethylamine (11.9 mL, 85.2 mmol) and diphenylphosphonic azide (18.4 mL, 85.2 mmol) were added and the reaction was heated at reflux for 18 hours. The reaction was evaporated to a residue. The residue was dissolved in ethyl acetate (250 mL) and washed with water (100 mL), 5% citric acid (aqueous, 100 mL), water (100 mL), saturated aqueous sodium bicarbonate (100 mL) and brine (100 mL). The organic phase was dried over magnesium sulfate and evaporated to a brown solid. The solid was purified by silica gel chromatography in 5%-40% ethyl acetate / hexane gradient elution to afford the title compound as a colorless solid (12.8 g, 77.4%). ^{1}H NMR (400 MHz, DMSO-d_6) δ ppm 1.45 (s, 9 H) 7.21 (br. s., 1 H) 8.87 (d, *J*=2.34 Hz, 1 H) 10.17 (br. s., 1 H). HPLC (12 min), t_R = 8.09 min, HPLC purity >95%. LCMS (ESI) *m/z* 201 $[M+H]^+$.

***tert*-Butyl ((5-chloro-2, 4-difluorophenyl) sulfonyl) (thiazol-4-yl) carbamate (44).** A THF (2 mL) solution of tert-butyl thiazol-4-ylcarbamate (**42**) (195 mg, 0.97 mmol) was treated with a solution of 1M LiHMDS in THF (972 μL, 0.97 mmol) at 0 ^{o}C and stirred for 30 minutes. Then, 5-chloro-2, 4-difluorobenzenesulfonyl chloride (**43**) (200 mg, 0.810 mmol) was added at 0 ^{o}C.

The mixture was allowed to warm to room temperature and stirred overnight. The mixture was treated with water (6 mL) and stirred for 1 hour. The resulting precipitate was filtered and purified by column chromatography eluting with a gradient of 100% heptanes to 50% EtOAc / heptanes to afford the title compound as a colorless solid (166 mg, 50%). ^{1}H NMR (400 MHz, $CDCl_3$) δ ppm 1.39 (s, 9 H) 7.10 (t, *J*=8.79 Hz, 1 H) 7.54 (d, *J*=2.15 Hz, 1 H) 8.25 (t, *J*=7.52 Hz, 1 H) 8.80 (d, *J*=2.15 Hz, 1 H). HPLC (6 min), t_R = 2.9 min, HPLC purity >95%. LCMS (ESI) *m/z* 411 $[M+H]^+$.

5-Chloro-N-(2,4-dimethoxybenzyl)-2,4-difluoro-N-1,3,4-thiadiazol-2-ylbenzenesulfonamide (47). To a suspension of the N-(2,4-dimethoxybenzyl)-1,3,4-thiadiazol-2-amine (**45**) (27.7 g, 110 mmol) in 2-methyl-THF (225 mL) at -45 ^{o}C was added dropwise a solution of LiHMDS (1M in THF, 121mL, 121 mmol) maintaining temp between -40 to -45 ^{o}C. After addition the heterogeneous mixture allowed to stir at -45 ^{o}C for 45 minutes. To the resultant suspension at -45 ^{o}C was added a 2-methyl-THF solution (45 mL) of 5-chloro-2,4-difluorobenzenesulfonyl chloride (**46**) (27.2 g, 110 mmol) at such a rate as to maintain the temp between -45 ^{o}C to -40 ^{o}C. After addition the resultant orange solution was allowed to warm to 0 ^{o}C over 2 hours. The reaction was quenched with a saturated aqueous ammonium chloride solution and extracted with EtOAc. The organic layers were washed with water and brine, dried over $MgSO_4$, before concentration in vacuo to give an oil. Purification was accomplished by flash chromatography eluting with 30-50% EtOAc/heptanes to provide the title compound as a pale yellow solid (39.9 g, 78%). ^{1}H NMR (500 MHz, $CDCl_3$) δ ppm 3.73 (s, 3 H) 3.78 (s, 3 H) 5.35 (s, 2 H) 6.29 (d, *J*=2.44 Hz, 1 H) 6.38 (dd, *J*=8.42, 2.32 Hz, 1 H) 6.98 (t, *J*=8.78 Hz, 1 H) 7.29 (d, *J*=2.68 Hz, 1 H) 7.84 (t, *J*=7.44 Hz, 1 H) 8.87 (s, 1 H). HPLC (5 min), t_R = 3.59 min, HPLC purity >95%. LCMS (ESI) *m/z,* 462 $[M+H]^+$.

2-Iodo-4-(trifluoromethyl) phenol (49). A mixture of iodine (23.2 g, 91.6 mmol), and sodium carbonate (7.7 g, 91.6 mmol,) was added to a solution of 4-(trifluoromethyl) phenol (**48**) (13.5 g, 83.3 mmol,) in THF (90 mL) and water (90 mL), then the reaction was allowed to stir at room temperature for 18 hours. Sufficient thiourea (5% solution) was added to remove the excess iodine, as indicated by the color change of the reaction from deep violet to brown. The reaction mixture was then extracted with diethyl ether. The organic phase was dried over $MgSO_4$, concentrated in vacuo to give brown oil. This was purified by silica gel chromatography (E_2O:Hexane = 1:10) followed by trituration with Et_2O/hexane to provide the title compound as a tan solid (9.84 g, 41%). ^{1}H NMR (400 MHz, $CDCl_3$) δ ppm 6.07 (s, 1 H) 7.94 (s, 2 H). HPLC (2 min), t_R = 1.53 min, HPLC purity >95%. LCMS (ESI) *m/z* 288.1 $[M+H]^+$.

2-Pyridazin-4-yl-4-(trifluoromethyl)phenol (51). To an argon flushed flask containing a solution of 4-(tributylstannyl)pyridazine (**50**) (5.0 g, 13.5 mmol) in acetonitrile (20 mL) was added 2-iodo-4-(trifluoromethyl)phenol, (**49**) (3.9 g, 13.5 mmol) in acetonitrile (30 mL). Copper iodide (500 mg, 2.63 mmol) was added followed by $Pd(PPh_3)_4$ (750 mg, 0.65 mmol) and cesium fluoride (4.1 g, 27 mmol). The mixture was heated to 50 ^oC for 2 hours and allowed to cool before concentrating in vacuo. The residue was partitioned between dichloromethane (50 mL) and aqueous 2M HCl (100 mL)/water (20 mL). The organic layer was re-extracted with aqueous 2M HCl (15 mL) and the combined aqueous extracts were neutralized by adding solid $NaHCO_3$ slowly. The mixture was then extracted with EtOAc (100 mL), dried over Na_2SO_4 and concentrated in vacuo to provide the title compound as a solid (2.2 g, 68%). ^{1}H NMR (400 MHz, DMSO-d_6) δ ppm 7.19 (d, *J*=8.40 Hz, 1 H) 7.68 (dd, *J*=8.69, 2.05 Hz, 1 H) 7.83 (d, *J*=1.76 Hz, 1 H) 7.95 (d, *J*=3.51 Hz, 1 H) 9.29 (br. s., 1 H) 9.52 (br. s., 1 H) 11.11 (s, 1 H). LCMS (ESI) *m/z* 241 $[M+H]^+$.

5-Chloro-N-(2,4-dimethoxybenzyl)-2-fluoro-4-[2-pyridazin-4-yl-4-(trifluoromethyl)phenoxy]-N-1,3,4-thiadiazol-2-ylbenzenesulfonamide (52). A stirred solution of the 2-pyridazin-4-yl-4-(trifluoromethyl) phenol (**51**) (890 mg, 3.7 mmol) in DMSO (10 mL) was treated with potassium carbonate (563 mg, 4.08 mmol) and the mixture stirred for 1 minute. Solid 5-chloro-N-(2,4-dimethoxybenzyl)-2,4-difluoro-N-1,3,4-thiadiazol-2-ylbenzenesulfonamide (**47**) (1.71 g, 3.7 mmol) was then added portion-wise and the reaction mixture stirred at room temperature for 18 hours. The reaction mixture was poured onto aqueous 1M NaOH (120 mL) and the resulting precipitate extracted with EtOAc (3 x 100 mL). The combined organic extracts were washed with water and dried over $MgSO_4$ to give a foam. Purification by flash column chromatography, eluting with a gradient of 50% EtOAc/heptane to 100% EtOAc gave the title compound as a foam (1.69 g, 67%). ^{1}H NMR (400 MHz, $CDCl_3$) δ ppm 3.71 (s, 3 H) 3.75 (s, 3 H) 5.33 (s, 2 H) 6.27 (d, *J*=2.15 Hz, 1 H) 6.36 (dd, *J*=8.40, 2.34 Hz, 1 H) 6.62 (d, *J*=9.76 Hz, 1 H) 7.07 (d, *J*=8.40 Hz, 1 H) 7.26 - 7.33 (m, 1 H partially obscured by chloroform) 7.71 (dd, *J*=5.27, 2.34 Hz, 1 H) 7.77 - 7.84 (m, 2 H) 7.87 (d, *J*=6.83 Hz, 1 H) 8.85 (s, 1 H) 9.31 (d, *J*=5.27 Hz, 1 H) 9.46 (s, 1 H). HPLC (2 min), t_R = 1.79 min, HPLC purity >95%. LCMS (ESI) *m/z* 682 $[M+H]^+$.

4-Chloro-2-{1-[1-(diphenylmethyl)azetidin-3-yl]-1H-pyrazol-5-yl} phenol (55). 1-(diphenylmethyl)-3-hydrazinoazetidine dihydrochloride (**54**) (1.00 g, 3.06 mmol) was added to an ice cold, stirred suspension of (2*E*)-1-(5-chloro-2-hydroxyphenyl)-3-(dimethylamino)prop-2-en-1-one (**53**) (700 mg, 3.1 mmol) in ethanol (5 mL) and acetic acid (5 mL), stirred at 0 °C for 2 hours then allowed to warm to room temperature over 2 hours. The solvents were removed in vacuo and the residue partitioned between ethyl acetate (80 mL) and saturated aqueous sodium hydrogen carbonate solution (50 mL). The organic layer was separated and dried over sodium

sulfate, filtered and the solvents removed in vacuo to give a yellow gum. This was dissolved in warm methyl-t-butyl ether (20 mL) and allowed to crystallize to provide the title compound as a pale yellow powder (541 mg, 42%). ^{1}H NMR (400 MHz, $CDCl_3$) δ ppm 3.63 (dd, *J*=7.52, 1.85 Hz, 4 H) 4.61 (s, 1 H) 4.86 (quin, *J*=7.47 Hz, 1 H) 6.33 (d, *J*=1.76 Hz, 1 H) 6.88 (d, *J*=8.79 Hz, 1 H) 7.08 (d, *J*=2.54 Hz, 1 H) 7.15 - 7.22 (m, 2 H) 7.23 - 7.35 (m, 5 H) 7.39 - 7.49 (m, 5 H) 7.70 (d, *J*=1.76 Hz, 1 H). HPLC (6 min), t_R = 1.27 min, HPLC purity >95%. LCMS (ESI) *m/z* 416 $[M+H]^+$.

***tert*-Butyl ((3-cyano-4-fluorophenyl)sulfonyl)(thiazol-4-yl)carbamate (57).** To a stirred solution of *tert*-butyl 1,3-thiazol-4-ylcarbamate (**42**) (0.500 g, 2.497 mmol) in tetrahydrofuran (10 mL) was added lithium 1,1,1,3,3,3-hexamethyldisilazan-2-ide (1.0 M solution in tetrahydrofuran, 2.50 mL, 2.5 mmol) at 0 °C under nitrogen. After stirring for 1 hour at 0 °C the reaction mixture was cooled to -78 °C and 3-cyano-4-fluorobenzenesulfonyl chloride (**56**) (0.453 g, 2.063 mmol) in tetrahydrofuran (5.0 mL) was added. The mixture was warmed to room temperature for 16 hours. Saturated aqueous ammonium chloride solution (20 mL) was added and the aqueous layer was extracted with ethyl acetate (3 x 20 mL). Combined organic layers were dried over sodium sulfate and concentrated *in vacuo*. This crude residue was purified by flash chromatography eluting with ethyl acetate:dichloromethane (gradient 0:1 to 3:7) to afford the title compound as a white solid (426 mg, 54%). ^{1}H NMR (400 MHz, DMSO-d_6) δ ppm 1.26 (s, 9 H) 7.91 (t, *J*=8.99 Hz, 1 H) 8.18 (d, *J*=2.34 Hz, 1 H) 8.45 (ddd, *J*=9.08, 4.79, 2.54 Hz, 1 H) 8.59 (dd, *J*=5.86, 2.34 Hz, 1 H) 9.18 (d, *J*=2.34 Hz, 1 H). LCMS (ESI) *m/z* 384 $[M+H]^+$.

***tert*-Butyl{[4-(4-chloro-2-{1-[1-(diphenylmethyl)azetidin-3-yl]-1*H*-pyrazol-5-yl}phenoxy)-3-cyanophenyl]sulfonyl}1,3-thiazol-4-ylcarbamate (58).** 4-chloro-2-{1-[1-(diphenylmethyl)azetidin-3-yl]-1*H*-pyrazol-5-yl}phenol, (**55**) (75 mg, 0.18 mmol), *tert*-butyl [(3-

cyano-4-fluorophenyl)sulfonyl]1,3-thiazol-4-ylcarbamate (**57**) (69 mg, 0.18 mmol), potassium carbonate (62 mg, 0.45 mmol) and dimethyl sulfoxide (4 mL) were combined and stirred at room temperature under nitrogen for 4 hours. Saturated aqueous ammonium chloride solution (20 mL) was added and the mixture extracted with ethyl acetate (20 ml). The organic layer was separated and back-washed with saturated aqueous sodium chloride solution (2 x 20 mL). The organic layer was separated, dried over sodium sulfate, filtered and evaporated to give an oil. The oil was purified by flash chromatography, eluting with a gradient from dichloromethane to dichloromethane: methanol (98:2) to provide the title compound as a glassy solid (33 mg, 24%). ^{1}H NMR (400 MHz, $CDCl_3$) δ ppm 1.32 (s, 9 H) 3.55 - 3.63 (m, 2 H) 3.64 - 3.71 (m, 2 H) 4.57 (s, 1 H) 4.92 (quin, *J*=7.22 Hz, 1 H) 6.22 (d, *J*=1.76 Hz, 1 H) 6.67 (d, *J*=8.98 Hz, 1 H) 7.11 - 7.22 (m, 4 H) 7.23 - 7.31 (m, 2 H) 7.34 (d, *J*=2.54 Hz, 1 H) 7.43 (d, *J*=7.22 Hz, 4 H) 7.47 - 7.55 (m, 3 H) 8.10 (dd, *J*=8.98, 2.34 Hz, 1 H) 8.31 (d, *J*=2.34 Hz, 1 H) 8.59 (d, *J*=2.15 Hz, 1 H). HPLC (6 min), t_R = 1.41 min, HPLC purity >95%. LCMS (ESI) *m/z* 779 $[M+H]^+$.

4-[2-(1-Azetidin-3-yl-1*H*-pyrazol-5-yl)-4-chlorophenoxy]-3-cyano-N-1,3-thiazol-4-ylbenzenesulfonamide (59). *tert*-butyl{[4-(4-chloro-2-{1-[1-(diphenylmethyl)azetidin-3-yl]-1*H*-pyrazol-5-yl}phenoxy)-3-cyanophenyl]sulfonyl}1,3-thiazol-4-ylcarbamate, (**58**) (224 mg, 0.287 mmol) was dissolved in dichloromethane (10 mL) and N,N,N',N'-tetramethylnaphthalene-1,8-diamine (150 mg, 0.70 mmol) was added, followed by 1-chloroethyl chloroformate (0.07 ml, 0.65 mmol) and the solution was stirred at room temperature for 3.5 hours. The mixture was concentrated in vacuo and the residue was dissolved in methanol (10 mL) and refluxed for 4 hours before concentrating in vacuo to give the crude title compound as a brown gum, as a mixture of 4-[2-(1-azetidin-3-yl-1H-pyrazol-5-yl)-4-chlorophenoxy]-3-cyano-N-1,3-thiazol-4-ylbenzenesulfonamide & *tert*-butyl ({4-[2-(1-azetidin-3-yl-1*H*-pyrazol-5-yl)-4-chlorophenoxy]-

3-cyanophenyl}sulfonyl)1,3-thiazol-4-ylcarbamate (200 mg crude). This mixture was stirred in 4M hydrogen chloride solution in 1,4-dioxane (10 mL) at room temperature for 2 hours. The reaction mixture was concentrated in vacuo and the residue was partitioned between methyl-*t*-butyl ether (80 mL) and water (40 mL) (neutralized to pH=7 with sodium hydrogen carbonate). The organic layer was then concentrated in vacuo and the crude product purified by column chromatography using dichloromethane:methanol:conc. ammonium hydroxide (90:10:1 to 70:30:3). This provided a buff powder (65 mg) which was triturated with methyl tert-butyl ether to provide the title compound as a beige powder (55 mg, 33%). ^{1}H NMR (400 MHz, DMSO-d_6) δ ppm 4.00 - 4.12 (m, 4 H) 5.04 - 5.12 (m, 1 H) 6.28 (d, *J*=1.56 Hz, 1 H) 6.37 (s, 1 H) 6.84 (d, *J*=8.97 Hz, 1 H) 7.41 (d, *J*=8.97 Hz, 1 H) 7.60 (dd, *J*=5.65, 2.14 Hz, 2 H) 7.67 (dd, *J*=8.78, 2.54 Hz, 1 H) 7.82 (dd, *J*=8.97, 1.95 Hz, 1 H) 7.99 (d, *J*=1.95 Hz, 1 H) 8.65 (d, *J*=2.34 Hz, 1 H)., HPLC (2 min), t_R = 1.26 min, HPLC purity >95%. LCMS (ESI) *m/z* 513 $[M^+H]^+$.

ASSOCIATED CONTENT

Supporting Information

Detailed syntheses, characterization, purity analysis and molecular formula strings of all compounds are disclosed. Electrophysiology protocols for ion channel in vitro profiling and secondary pharmacology data is also outlined. This material is available free of charge via the Internet at http://pubs.acs.org.

Accession Code

Coordinates and structure factors have been submitted to the PDB under accession code 5K7K for compound **29** bound to CYP2C9. Authors will release the atomic coordinates and experimental data upon article publication.

AUTHOR INFORMATION

Corresponding Author

*To whom correspondence should be addressed. Tel +44 (0)1707 358693. E-mail: nigel.swain@heptares.com.

Present Addresses

† (N.A.S.) Heptares Therapeutics Ltd, BioPark, Broadwater Road, Welwyn Garden City, AL7 3AX, United Kingdom. (R.I.S. and A.P.) AstraZeneca, Darwin Building, 310 Cambridge Science Park, Milton, Cambridge, CB4 0FZ, United Kingdom.

Author Contributions

The manuscript was written through contributions of all authors who have given approval for publication of the manuscript.

Notes

The authors declare no competing financial interest.

ACKNOWLEDGMENT

We acknowledge PeakDale Molecular (Concept Life Sciences) for synthetic support, Jill Chrencik for CYP2C9 structure PDB deposition and Rubben Torella for the CYP2C9 graphic. We also thank Raj Logan for the Pharmacokinetic, Dynamics and Metabolism screening support.

ABBREVIATIONS

ADME, Absorption Distribution Metabolism Excretion; AUC, area under curve; Boc, tert-butyloxycarbonyl; Cl_{int}, intrinsic clearance; C_{max}, maximum concentration; Cl_p, plasma clearance; Cl_u, unbound clearance; CYP, cytochrome P450; DDI, drug-drug interaction; DLM, dog liver microsomes; DMB di-methoxy benzyl; F, bioavailability; F_u, fraction unbound; HBA, H-bond acceptor; HBD, H-bond donor; hep, hepatocytes; HET, heterocycle; HLM, human liver microsomes; IV, intravenous; LHS, left hand side; LipE, lipophilic efficiency; MDCK-MDR1, Madin-Darby canine kidney, multi-drug resistance; OATP, organic anion-transporting polypeptide; P_{app}, apparent permeability; PK, pharmacokinetics; PPB, plasma protein binding; RHS, right hand side; RLM, rat liver microsomes; RRCK, Ralph Russ canine kidney; SAR, structure activity relationship; $T_{1/2}$, plasma half-life; T_{max}, time at maximum plasma concentration; TPSA, topological polar surface area; V_{ss}, volume of distribution (steady state).

REFERENCES

(1) (a) Goldin, A. L, Resurgence of sodium channel research. *Ann. Rev. Physiol.* **2001**, *63*, 871-894. (b) Wood, J. N.; Boorman, J. Voltage-gated sodium channel blockers; target validation and therapeutic potential. *Curr. Top. Med. Chem.* **2005**, *5*, 529-537.

(2) (a) Bagal, S. K.; Brown, A. D.; Cox, P. J.; Omoto, K.; Owen, R. M.; Pryde, D. C.; Sidders, B.; Skerratt, S. E.; Stevens, E. B.; Storer, R. I.; Swain, N. A. Ion channels as therapeutic targets: a drug discovery perspective. *J. Med. Chem.* **2013**, *56*, 593-624. (b) Bagal, S. K.; Chapman, M. L.; Marron, B. E.; Prime, R.; Storer, R. I.; Swain, N. A.. Recent progress in sodium channel modulators for pain. *Bioorg. Med. Chem. Lett.* **2014**, *24*, 3690-3699.

(3) Eijkelkamp, N.; Linley, J. E.; Baker, M. D.; Minett, M. S.; Cregg, R.; Werdehausen, R.; Rugiero, F.; Wood, J. N. Neurological perspectives on voltage-gated sodium channels. *Brain* **2012**, *135*, 2585-2612.

(4) (a) Dib-Hajj, S. D.; Yang, Y.; Black, J. A.; Waxman, S. G. The $Na_V1.7$ sodium channel: from molecule to man. *Nat. Rev. Neurosci.* **2013**, *14*, 49-62. (b) Waxman, S. G.; Zamponi, G. W. Regulating excitability of peripheral afferents: emerging ion channel targets. *Nat. Neurosci.* **2014**, *17*, 153-163. (c) Gingras, J.; Smith, S.; Matson, D. J.; Nye, D.; Couture, L.; Feric, E.; Yin, R.; Moyer, B. D.; Peterson, M. L.; Rottman, J. B.; Beiler, R. J.; Malmberg, A. B.; McDonough, S. I. Global $Na_V1.7$ knockout mice recapitulate the phenotype of human congenital indifference to pain. *PLoS One* **2014**, *9*, e105895.

(5) (a) Cox J. J.; Reimann F.; Nicholas A. K.; Thornton, G.; Roberts, E.; Springell, K.; Karbani, G.; Jafri, H.; Mannan, J.; Raashid, Y.; Al-Gazali, L.; Hamamy, H.; Valente, E. M.; Gorman, S.; Williams, R.; McHale, D. P.; Wood, J. N.; Gribble, F. M.; Woods, G. C. An SCN9A channelopathy causes congenital inability to experience pain. *Nature* **2006**, *444*, 894-898. (b) Goldberg Y. P.; MacFarlane J.; MacDonald M. L.; Thompson J.; Dube, M. P.; Mattice, M.; Fraser, R.; Young, C.; Hossain, S.; Pape, T.; Payne, B.; Radomski, C.; Donaldson, G.; Ives, E.; Cox, J.; Younghusband, H. B.; Green, R.; Duff, A.; Bolthauser, E.; Grinspan, G. A.; Dimon, J. H.; Sibley, B. G.; Andria, G.; Toscano, E.; Kerdraon, J.; Bowsher, D.; Pimstone, S. N.; Samuels, M. E.; Sherrington, R.; Hayden, M. R. Loss-of-function mutations in the $Na_V1.7$ gene underlie congenital indifference to pain in multiple human populations. *Clin. Genet.* **2007**, *71*, 311-319.

(6) (a) Fertleman C. R.; Baker M. D.; Parker K. A.; Moffatt S.; Elmslie, F. V.; Abrahamsen, B.; Ostman, J.; Kluqbauer, N.; Wood, J. N.; Gardiner, R. M.; Rees, M. SCN9A mutations in paroxysmal extreme pain disorder: allelic variants underlie distinct channel defects and phenotypes. *Neuron* **2006**, *52*, 767-774. (b) Yang Y.; Wang Y.; Li S.; Xu, Z.; Li, H.; Ma, L.; Fan, J.; Bu, D.; Fan, Z.; Wu, G.; Jin, J.; Ding, B.; Zhu, X.; Shen, Y. Mutations in SCN9A, encoding a sodium channel alpha subunit, in patients with primary erythermalgia. *J. Med. Genet.*

2004, *41*, 171-174. (c) Drenth J. P.; te Morsche R. H.; Guillet, G.; Taieb, A.; Kirby, R. L.; Jansen, J. B. SCN9A mutations define primary erythermalgia as a neuropathic disorder of voltage gated sodium channels. *J. Invest. Dermatol.* **2005**, *124*, 1333-1338.

(7) (a) Nardi, A.; Damann, N.; Hertrampf, T.; Kless, A. Advances in targeting voltage-gated sodium channels with small molecules. *ChemMedChem*. **2012**, *7*, 1712-1740. (b) de Lera, R. M.; Kraus, R. L. J. Voltage-gated sodium channels: Structure, function, pharmacology, and clinical indications. *J. Med. Chem.* **2015**, *58*, 7093-7118. (c) King, G. F.; Vetter, I. No gain, no pain: $Na_V1.7$ as an analgesic target. *ACS Chem. Neurosci.* **2014**, *5*, 749-751.

(8) Beaudoin, S.; Laufer-Sweiler, M. C.; Markworth, C. J.; Marron, B. E.; Millan, D. S.; Rawson, D. J.; Reister, S. M.; Sasaki, K.; Storer, R. I.; Stupple, P. A.; Swain, N. A.; West, C. W.; Zhou, S. Sulfonamide derivatives. PCT Int. Appl. WO2010079443, Jul 15, 2010.

(9) McCormack, K.; Santos, S.; Chapman, M. L.; Krafte, D. S.; Marron, B. E.; West, C. W.; Krambis, M. J.; Antonio, B. M.; Zellmer, S. G.; Printzenhoff, D.; Padilla, K.; M.; Lin, Z.; Wagoner, P. K.; Swain, N. A.; Stupple, P. A.; de Groot, M.; Butt, R. P.; Castle, N. A. Voltage sensor interaction site for selective small molecule inhibitors of voltage-gated sodium channels. *Proc. Natl. Acad. Sci. U. S. A.* **2013**, *110*, E2724-E2732.

(10) Ahuja, S.; Mukund, S.; Deng, L.; Khakh, K.; Chang, E.; Ho, H.; Shriver, S.; Young, C.; Lin, S.; Johnson, J. P.; Wu, P.; Li, J.; Coons, M.; Tam, C.; Brillantes, B.; Sampang, H.; Mortara, K.; Bowman, K. K.; Clark, K. R.; Estevez, A.; Xie, Z.; Verschoof, H.; Grinwood, M.; Dehnhardt, C.; Andrez, J-C.; Focken, T.; Sutherlin, D. P.; Safina, B. S.; Starovasnik, M. A.; Ortwine, D. F.; Franke, Y.; Cohen, C. J.; Hackos, D. H.; Koth, C. M.; Payandeh, J. Structural basis of $Na_V1.7$ inhibition by an isoform-selective small-molecule antagonist. *Science* **2015**, *350*, 1491.

(11) Payandeh J.; Scheuer T.; Zheng N.; Catterall W. A. The crystal structure of a voltage-gated sodium channel. *Nature*, **2011**, *475*, 353-358.

(12) (a) Sun, S.; Cohen, C. J.; Dehnhardt C. M. Inhibitors of voltage-gated sodium channel $Na_V1.7$: patent applications since 2010. *Pharm. Pat. Anal.* **2014**, *3*, 509-521. (b) Sun, S.; Jia, Q.; Zenova, A, Y,; Chafeev, M.; Zhang, Z,; Lin, S.; Kwan, R.; Grimwood, M. E.; Chowdhury, S.; Young, C.; Cohen, C. J.; Oballa, R. M; The discovery of benzenesulfonamide-based potent and selective inhibitors of voltage-gated sodium channel $Na_V1.7$. *Bioorg. Med. Chem Lett.* **2014**, *24*, 4397-4401. (c) Focken, T.; Liu, S.; Chahal, N.; Dauphinais, M.; Grimwood, M. E.; Chowdhury, S.; Hemeon, I.; Bichler, P.; Bogucki, D.; Waldbrook, M.; Bankar, G.; Sojo, L. E.; Young, C.; Lin, S.; Shuart, N.; Kwan, R.; Pang, J.; Chang, J. H.; Safina, B. S.; Sutherlin, D. P.; Johnson, Jr. J. P.; Dehnhardt, C. M.; Mansour, T. S.; Oballa, R. M.; Cohen, C. J.; Robinette, C. L. Discovery of aryl sulfonamides as isoform-selective inhibitors of $Na_V1.7$ with efficacy in rodent pain models. *ACS Med. Chem. Lett.* **2016**, *7*, 277-282. (d) DiMauro, E. F.; Altmann, S.; Berry, L. M.; Bregman, H.; Chakka, N.; Chu-Moyer, M.; Bojic, E F; Foti, Robert S.; Fremeau, R.; Gao, H.; Gunaydin, H.; Guzman-Perez, A.; Hall, B. E.; Huang, H.; Jarosh, M.; Kornecook, T.; Lee, J.; Ligutti, J.; Liu, D.; Moyer, B. D.; Ortuno, D.; Rose, P. E.; Schenkel, L. B.; Taborn, K.; Wang, J.; Wang, Y.; Yu, V.; Weiss, M. M. Application of a parallel synthetic strategy in the discovery of biaryl acyl sulfonamides as efficient and selective $Na_V1.7$ inhibitors. *J. Med. Chem.* **2016**, *59*, 7818-7839. (e) Marx, I. E.; Dineen, T. A.; Able, J.; Bode, C.; Bregman, H.; Chu-Moyer, M.; Di Mauro, E. F.; Du, B.; Foti, R. S.; Fremeau, R. T.; Gao, H.; Gunaydin, H.; Hall, B. E.; Huang, L.; Kornecook, T.; Kreiman, C. R.; La, D. S.; Ligutti, J.; Lin, M. J.; Liu, D.; McDermott, J. S.; Moyer, B. D.; Peterson, E. A.; Roberts, J. T.; Rose, P.; Wang, J.; Youngblood, B. D.; Yu, V. L.; Weiss, M. M. Sulfonamides as selective $Na_V1.7$ inhibitors: Optimizing potency and

pharmacokinetics to enable in vivo target engagement. *ACS Med. Chem. Lett.* **2016**, *7*, 1062-1067. (f) Wu, Y.; Guernon, J.; Shi, J.; Ditta, J.; Robbins, K. J.; Rajamani, R.; Easton, A.; Newton, A.; Bourin, C.; Mosure, K.; Soars, M. G.; Knox, R. J.; Matchett, M.; Pieschl, R. L.; Post-Munson, D. J.; Wang, S.; Herrington, J.; Graef, J.; Newberry, K.; Bristow, L. J.; Meanwell, N. A.; Olson, R.; Thompson, L. A.; Dzierba, C. Development of new benzenesulfonamides as potent and selective $Na_V1.7$ inhibitors for the treatment of pain. *J. Med. Chem.* **2017**, *60*, 2513-2525. (g) Sparling, B. A.; Yi, S.; Able, J.; Bregman, H.; DiMauro, E. F.; Foti, R. S.; Gao, H.; Guzman-Perez, A.; Huang, H.; Jarosh, M.; Kornecook, T.; Ligutti, J.; Milgram, B. C.; Moyer, B. D.; Youngblood, B.; Yu, V. L.; Weiss, M. M. Discovery and hit-to-lead evaluation of piperazine amides as selective, state-dependent $Na_V1.7$ inhibitors. *Med. Chem. Commun.* **2017**, *8*, 744-754. (h) Weiss, M. M.; Dineen, T. A.; Marx, I. E.; Altmann, S.; Boezio, A. A.; Bregman, H.; Chu-Moyer, M. Y.; Di Mauro, E. F.; Bojic, E. F.; Foti, R. S.; Gao, H.; Graceffa, R. F.; Gunaydin, H.; Guzman-Perez, A.; Huang, H.; Huang, L.; Jarosh, M.; Kornecook, T.; Kreiman, C. R.; Ligutti, J.; La, D. S.; Lin, M. J.; Liu, D.; Moyer, B. D.; Nguyen, H. N.; Peterson, E. A.; Rose, P. E.; Taborn, K.; Youngblood, B. D.; Yu, V. L.; Fremeau, R. T., Jr. Sulfonamides as selective $Na_V1.7$ inhibitors: Optimizing potency and pharmacokinetics while mitigating metabolic liabilities. *J. Med. Chem.* [Online early access]. DOI: 10.1021/acs.jmedchem.6b01851. Published Online: Mar 13, 2017. http://pubs.acs.org/doi/abs/10.1021/acs.jmedchem.6b01851 (accessed Jun 14 2017). (i) Graceffa, R. F.; Boezio, A. A.; Able, J.; Altmann, S.; Berry, L. M.; Boezio, C. M.; Butler, J. R.; Chu-Moyer, M. Y.; Cooke, M.; Di Mauro, E. F.; Dineen, T. A.; Bojic, F. E.; Foti, R. S.; Fremeau, R. T., Jr.; Guzman-Perez, A.; Gao, H.; Gunaydin, H.; Huang, H.; Huang, L.; Ilch, C.; Jarosh, M.; Kornecook, T.; Kreiman, C. R.; La, D. S.; Ligutti, J.; Milgram, B. C.; Lin, M. J.; Marx, I. E.; Nguyen, H. N.; Peterson, E. A.; Rescourio, G.; Roberts, J.; Schenkel, L. B.;

Shimanovich, R.; Sparling, B. A.; Stellwagen, J.; Taborn, K.; Vaida, K. R.; Wang, J.; Yeoman, J. T. S.; Yu, V. L.; Zhu, D.; Moyer, B. D.; Weiss, M. M. Sulfonamides as selective $Na_V1.7$ inhibitors: Optimizing potency, pharmacokinetics, and metabolic properties to obtain atropisomeric quinolinone (AM-0466) that affords robust in vivo activity. *J. Med. Chem.* [Online early access]. DOI: 10.1021/acs.jmedchem.6b01850. Published Online: Mar 21, 2017. http://pubs.acs.org/doi/abs/10.1021/acs.jmedchem.6b01850 (accessed Jun 14 2017).

(13) Stepan, A. F.; Walker, D. P.; Bauman, J.; Price, D. A.; Baillie, T. A.; Kalgutkar, A. S.; Aleo, M. D. Structural alert/reactive metabolite concept as applied in medicinal chemistry to mitigate the risk of idiosyncratic drug toxicity: a perspective based on the critical examination of trends in the top 200 drugs marketed in the United States. *Chem. Res. Toxicol.* **2011**, *24*, 1345-1410.

(14) Castle, N.; Printzenhoff, D.; Zellmer, S.; Antonio, B.; Wickenden, A.; Silvia, C. Sodium channel inhibitor drug discovery using automated high throughput electrophysiology platforms. *Comb. Chem. High Throughput Screening* **2009**, *12*, 107-122.

(15) Grime, K.; Paine, S. W. Species differences in biliary clearance and possible relevance of hepatic uptake and efflux transporters involvement. *Drug Metab. Dispos.* **2013**, *41*, 372-378.

(16) Jones, H. M.; Butt, R. P.; Webster, R. W.; Gurrell, I.; Dzygiel, P.; Flanagan, N.; Fraier, D.; Hay, T.; Iavarone, L. E.; Luckwell, J.; Pearce, H.; Phipps, A.; Segelbacher, J.; Speed, B.; Beaumont, K. Clinical micro-dose studies to explore the human pharmacokinetics of four selective inhibitors of human $Na_V1.7$ voltage-dependent sodium channels. *Clin. Pharmacokinet.* **2016**, *55*, 875–887.

(17) (a) Alexandrou, A. J.; Brown, A. R.; Turner, J.; Mis, M. A.; Wilbrey, A.; Payne, E. C.; Gutteridge, A.; Cox, P. J.; Butt, R. P.; Stevens, E. B.; Chapman, M. L.; Printzenhoff, D.; Lin, Z.; Marron, B. E.; West, C.; Castle, N. A.; Krafte, D.; Estacion, M.; Dib-Hajj, S. D.; Waxman, S. G.; Doyle, R.; Swain, N. A.; Storer, R. I.; Stupple, P. A.; Hounshell, J. A.; Rivara, M.; Patel, M. K.; Randall, A.. Subtype-selective small molecule inhibitors reveal a fundamental role for $Na_V1.7$ in nociceptor electrogenesis, axonal conduction and presynaptic release. *PLoS One*, **2016**, *11*, e0152405. (b) Theile, J. W.; Fuller, M. D.; Chapman, M. L., The selective $Na_V1.7$ inhibitor, PF-05089771, interacts equivalently with fast and slow inactivated Nav1.7 channels. *Mol. Pharm.* **2016**, *90*, 540-548.

Insert Table of Contents Graphic and Synopsis Here